

The solutions to the differential eqs 18 and 19 are

$$[\text{Ar}^+, \text{T}^-] = C_1 \exp(\lambda_+ t) + C_2 \exp(\lambda_- t) \quad (20)$$

$$[\text{Ar}^+ // \text{T}^-] = (C_1/k_{-2})[\lambda_+ + k_1 + k_2] \exp(\lambda_+ t) + (C_2/k_{-2})[\lambda_- + k_1 + k_2] \exp(\lambda_- t) \quad (21)$$

where C_1 , C_2 , λ_+ , and λ_- are the rate constant terms given in the text (with eq 13). Since $(\text{Abs})_t = [\text{Ar}^+, \text{T}^-] + [\text{Ar}^+ // \text{T}^-]$, the time-dependent absorbance change is given in eq 13.

For Scheme IV, the effect of salt is included in the rate expression as

$$\frac{d[\text{Ar}^+, \text{T}^-]}{dt} = -(k_1 + k_2 + k_x[\text{salt}])([\text{Ar}^+, \text{T}^-]) \quad (22)$$

$$\frac{d[\text{Ar}^+ // \text{X}^-]}{dt} = k_x[\text{salt}][\text{Ar}^+, \text{T}^-] \quad (23)$$

in addition to the k_1 and k_2 terms given above. [The reverse of

eq 15 is neglected since the SSIP is more stable than the CIP and $[\text{TBA}^+\text{P}^-] \gg [\text{TBA}^+\text{T}^-]$. Integration gives the time-dependent variation in concentration as

$$[\text{Ar}^+, \text{T}^-] = \exp[-(k_1 + k_2 + k_x[\text{salt}])t] \quad (24)$$

$$[\text{Ar}^+ // \text{T}^-] = k_2\{k_1 + k_2 + k_x[\text{salt}]\}^{-1}\{1 - \exp[-(k_1 + k_2 + k_x[\text{salt}])t]\} \quad (25)$$

$$[\text{Ar}^+ // \text{X}^-] = k_x[\text{salt}]\{k_1 + k_2 + k_x[\text{salt}]\}^{-1}\{1 - \exp[-(k_1 + k_2 + k_x[\text{salt}])t]\} \quad (26)$$

Since $(\text{Abs})_t = [\text{Ar}^+, \text{T}^-] + [\text{Ar}^+ // \text{T}^-] + [\text{Ar}^+ // \text{X}^-]$, the time-dependent absorbance change is eq 14.

Registry No. ArNTNO₂, 91452-21-0; ArCTNO₂, 91452-20-9; ArFTNO₂, 91452-22-1; ArBTNO₂, 91452-19-6; ArHTNO₂, 36301-08-3; ArVTNO₂, 96689-10-0; ArMTNO₂, 140225-65-6.

Chiral Molecular Recognition in Monolayers of Diastereomeric *N*-Acylamino Acid Methyl Esters at the Air/Water Interface

Jonathan G. Heath and Edward M. Arnett*

Contribution from the Gross Chemical Laboratory, Department of Chemistry, Duke University, Durham, North Carolina 27706. Received December 23, 1991

Abstract: This article continues our study of the effects of headgroup geometry and temperature on chiral recognition in the force-area isotherms, thermodynamics of spreading, and surface shear viscosities of monolayers and mixed monolayers of long-chain amino acid ester surfactants. *N*-Stearoyl—and lauroyl—derivatives of the methyl esters of cysteine, cystine, and threonine are compared to the previously-reported serine derivative. The structural points at issue are as follows: (a) the effects of replacing the hydroxyl group of serine with the thiol group of cysteine; (b) the effect of joining two cysteine groups through their sulfur atoms to produce the two-chain cystine surfactant; and (c) the effect of attaching a methyl group to the carbon bearing the hydroxyl group in stearoylserine methyl ester (SSME) to produce the bulkier stearoylthreonine methyl ester (STME). Comparison is first made for the melting point versus enantiomer composition of the crystals for each compound. In all four cases a racemate is formed. Next, the corresponding effects of enantiomeric composition versus the appropriate surface properties are presented and behavior similar to the melting point curves is seen, implying stereoselective behavior when the monolayers are in equilibrium with their crystals or quasicrystalline condensed surface phases. Diastereomeric effects were small, since *meso*-dilauroylcystine dimethyl ester (DLCDME) showed properties which were nearly identical to its *D* and *L* enantiomers, and the *allo* form of STME was similar to its enantiomers. All four compounds showed distinctly different force-area curves for their enantiomers versus their racemic mixtures, but the shapes of the curves and phase behavior (between liquid-expanded and liquid-condensed films) depended heavily on temperature. All force-area curves show hysteresis effects in the difference between the compression and expansion regions, indicating, as we have shown before, that relaxation of compressed monolayer states is slow and that the films are in metastable states. Phase behavior is an erratic function of headgroup and temperature. Also, there is no general pattern of whether racemates or enantiomers are most expanded. No crystals of quality sufficient for X-ray analysis could be grown, so rigorous interpretation of properties and behavior in terms of structure cannot be made. However, clear differences between the behavior of stearoylcysteine methyl ester (SCME) and SSME can be interpreted in terms of hydrogen bonding of the serine hydroxyl group to the water subphase. Furthermore, comparison of force-area curves for a series of diastereomeric mixtures of *L*-STME and *L-*allo**-STME with *D*- and *L*-SSME suggests that the stereochemistry at the carbon between the ester and amide functions is primarily responsible for the stereoselectivity in the packing of STME films. Films of SCME were too condensed to allow a surface viscosity study, but those of DLCDME and STME exhibited Newtonian flow with essentially no stereoselectivity in their flow properties.

Introduction

There is a rapidly growing appreciation of the importance of intermolecular forces in determining chemical reactivity in a wide variety of systems of condensed matter, with much current interest in the "molecular recognition" factors that are responsible for the extraordinary selectivity and catalytic power of enzymes.¹⁻⁴

Stereochemistry is the most sensitive tool for probing the structural details of how molecules "see" each other as they come together to form complexes and transition states.

The elegant techniques of surface chemistry developed by Irving Langmuir and his colleagues for manipulating monolayer films at the air/water interface provide a unique means not only to measure intermolecular forces quantitatively but to control them at will. However, despite a considerable history of research which has explored the relationships between the structures of surfactants

(1) Breslow, R. *Pure Appl. Chem.* **1990**, *62*, 1859.

(2) Lehn, J.-M. *Angew. Chem., Int. Ed. Engl.* **1990**, *29*, 1304.

(3) Ikeura, Y.; Kurihara, K.; Kunitake, T. *J. Am. Chem. Soc.* **1991**, *113*, 7342.

(4) Rebek, J., Jr. *Angew. Chem., Int. Ed. Engl.* **1990**, *29*, 245.

and their surface properties,⁵ there was no concerted effort to combine the disciplines of stereochemistry with monolayer techniques until we initiated such an investigation in the late 1970s through a study of the properties of chiral monolayers.⁶ Subsequent work has shown that chiral discrimination between films of pure enantiomers and their racemates is highly dependent on such variables as headgroup structure, film pressure, temperature, and the nature of the subphase.⁷⁻¹⁰ Not surprisingly, diastereomeric interactions between the antipodes of different chiral surfactants can also be pronounced and quite selective.⁸ Perhaps surprisingly, monolayers of phospholipids have shown very little stereoselective recognition in monolayers.¹¹

Most of our work has employed long-chain, acyl derivatives of amino acid esters as the surfactant film-formers because of the ready accessibility of both enantiomers of a variety of amino acids. More recently, we examined a series of diastereomeric DL and meso two-chain ketones and demonstrated pronounced differences between their surface properties (force-area isotherms and surface viscosities) depending on the position of the carbonyl group linking the two chains.¹²

Of the various acylamino acid esters, stearoylserine methyl ester (SSME) has shown the greatest degree of chiral discrimination between the properties of its pure enantiomeric films and those of the corresponding racemate⁹ or of its diastereomeric combinations with other surfactants.⁸ The present article pursues the effects of structure in the acylamino acid methyl ester series by further elaboration of structure of the carbon to which the hydroxymethyl group is attached in SSME. Specifically, the hydroxyl group is replaced with a sulfhydryl function in stearoyl-cysteine methyl ester (SCME), which in turn is converted into the two-chain series of D-, L-, and *meso*-dilauroylcystine dimethyl ester (DLCDME) by oxidation of the thiol functionality. Comparisons are made between the surface properties of the free-floating single-chain cysteine surfactant and those of the corresponding two-chain cystine diastereomers, which may be considered as equivalent to bringing a pair of corresponding cysteine isomers face to face through their sulfur atoms.

Finally, the behavior of the SSME, SCME, and DLCDME films is compared with that of the diastereomeric monolayers of stearoylthreonine methyl esters, D-, L-, and *allo*-STME. For reference, the structures of these compounds are summarized on Figure 1, and following this they will be referred to by their acronyms.

As before, the properties to be reported will be the force-area (π -A) isotherms at several temperatures, the equilibrium spreading pressures (ESPs), and the surface shear viscosities obtained with a previously described canal viscometer.¹² The results clearly demonstrate that molecular recognition (i.e., chiral discrimination) is fairly dependent on the detailed stereochemistry of the headgroup and is manifested (for the STME films) primarily during the surface phase transition from "liquid-expanded" (LE) to "liquid-condensed" (LC) films.

Experimental Section

General Surface Laboratory Procedures. The practice of monolayer chemistry requires scrupulously clean conditions in order to obtain reproducible results, since monolayer films are notoriously sensitive to contamination.¹³ Toward this end, all experiments were performed in

(5) See: Gaines, G. L., Jr. *Insoluble Monolayers at Liquid-Gas Interfaces*; Interscience Publishers: New York, 1966, and references therein.

(6) Arnett, E. M.; Chao, J.; Kinzig, B.; Stewart, M.; Thompson, O. *J. Am. Chem. Soc.* **1978**, *100*, 5575.

(7) Arnett, E. M.; Chao, J.; Kinzig, B.; Stewart, M.; Thompson, O.; Verbiar, R. *J. Am. Chem. Soc.* **1982**, *104*, 389.

(8) Verbiar, R. Ph.D. Dissertation, Duke University, Durham, NC, 1983.

(9) Harvey, N. G.; Mirajovsky, D.; Rose, P. L.; Verbiar, R.; Arnett, E. M. *J. Am. Chem. Soc.* **1989**, *111*, 1115.

(10) Harvey, N. G.; Rose, P. L.; Mirajovsky, D.; Arnett, E. M. *J. Am. Chem. Soc.* **1990**, *112*, 3547.

(11) (a) Arnett, E. M.; Gold, J. M. *J. Am. Chem. Soc.* **1982**, *104*, 636.

(b) Gold, J. M. Ph.D. Dissertation, Duke University, Durham, NC, 1982.

(12) Harvey, N.; Rose, P.; Porter, N. A.; Huff, J. B.; Arnett, E. M. *J. Am. Chem. Soc.* **1988**, *110*, 4395.

(13) Reference 5, p 39.

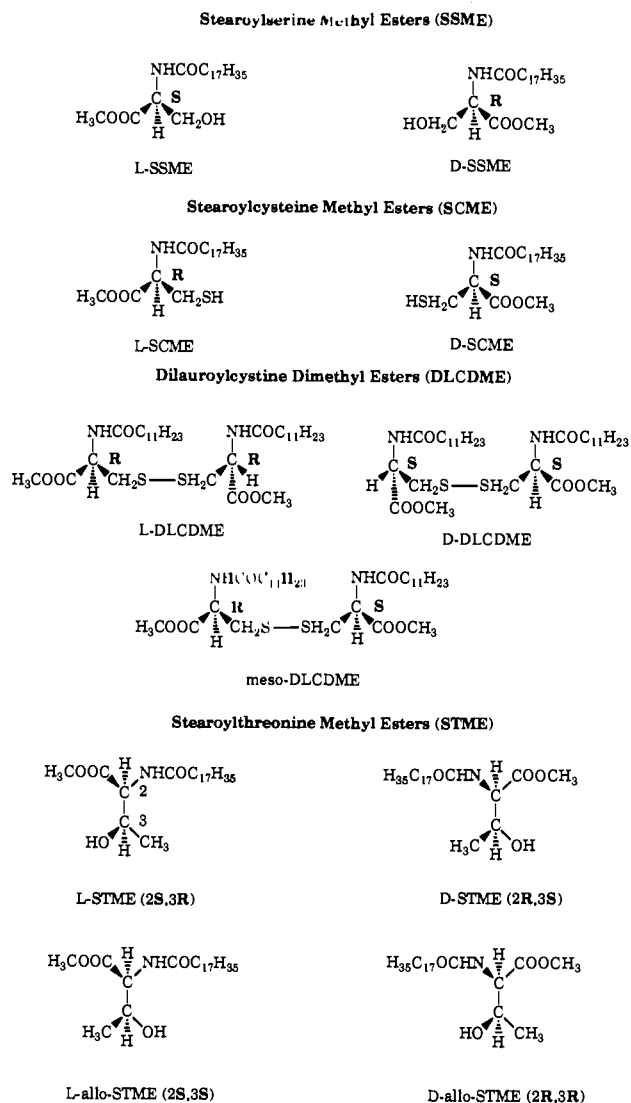


Figure 1. Structures of chiral surfactants.

a laboratory specifically dedicated to this project. All equipment and glassware were purchased new for this work and were never exposed to the environment outside the indicated laboratory. The cleanliness of the laboratory and equipment was ensured by the maintenance protocols described in previous publications.^{7,11} Likewise, the purification of all solvents and water has been described in detail.^{7,12}

These procedures may seem overinvolved, but the importance of cleanliness in monolayer work can hardly be exaggerated. Experience has shown that even trace quantities of impurities can lead to spurious results.¹⁴

Melting points were determined on a Thomas-Hoover melting point apparatus and corrected. Thin-layer chromatography was performed on glass silica gel plates (Sigma, No. T-6270) using ACS-certified solvents and developed in an iodine chamber. NMR spectra were collected on either a Varian XL-300 or a GE QE-300 spectrometer. IR spectra were obtained on a Bomem MB100 FTIR instrument. Optical rotations were determined using a Perkin-Elmer 241 polarimeter with cells of path length 1.000 ± 0.001 dm. Elemental analyses were done by M-H-W Laboratories, Phoenix, AZ.

The IR and NMR spectra of all products confirm their presumed structures and are given in detail in the doctoral thesis of J.G.H.¹⁵

Materials Preparation and Purification: Stearoylcysteine Methyl Esters. The stearoylcysteine methyl esters (L, D, and DL isomers) were prepared starting with the corresponding free amino acids (L-cysteine, Sigma No. C 7755, D-cysteine, Sigma No. C 8882, or DL-cysteine, Sigma No. 4022). Each amino acid (~3 g) was suspended in ~60 mL of

(14) Arnett, E. M.; Harvey, N. G.; Johnson, E. A.; Johnston, D. S.; Chapman, D. *Biochemistry* **1986**, *25*, 5239.

(15) Heath, J. G. Ph.D. Dissertation, Duke University, Durham, NC, 1991.

absolute methanol, which was obtained by distillation of methanol (Mallinckrodt, chromAR HPLC, No. 3041) from $\text{Mg}(\text{OCH}_3)_2$ using the method of Lund and Bjerrum¹⁶ under an atmosphere of scrubbed nitrogen. HCl gas (made from concentrated H_2SO_4 and NaCl, Mallinckrodt AR, No. 7581) was bubbled into the stirred suspension until dissolution took place. The solution was allowed to stand under scrubbed nitrogen for 12 h. The solvent was then removed to yield the amino acid methyl ester hydrochloride. The ester was coupled with stearoyl chloride (99%, Aldrich No. 17115-8) according to the method of Zeelen and Havinga.¹⁷

The product was purified by repeated recrystallization from methanol, which was distilled as described above. Recrystallizations were done in a glove bag filled with nitrogen to prevent the air oxidation of the thiol surfactant to the disulfide, and the product was dried in vacuo at 50 °C for 24 h. It was then stored under nitrogen in a refrigerator.

L-(+)-Stearoylcysteine methyl ester: mp 86.2–87.0 °C (lit.¹⁷ mp 85.5–87.0 °C); TLC (1/1 hexanes/EtOAc) $R_f = 0.55$; $[\alpha]_D^{20} = +32.1 \pm 0.3^\circ$ ($c = 0.56$ g/mL, CHCl_3). Anal. Calcd: C, 65.79; H, 10.79; N, 3.49; S, 7.98. Found: C, 65.89; H, 10.60; N, 3.27; S, 8.13.

D-(–)-Stearoylcysteine methyl ester: same data as for the L-(+) isomer except $[\alpha]_D^{20} = -32.2 \pm 0.2^\circ$ ($c = 0.56$ g/mL, CHCl_3). Anal. Found: C, 65.85; H, 10.70; N, 3.47; S, 8.11.

DL-(+)-Stearoylcysteine methyl ester: same data as for the L-(+) isomer except mp 64.5–65.5 °C; $[\alpha]_D^{20}$, no rotation detected. Anal. Found: C, 65.45; H, 10.53; N, 3.31.

Lauroylcysteine Methyl Esters. The cysteine methyl ester hydrochlorides were prepared as above and coupled to lauroyl chloride (98%, Aldrich No. 15693-0). They were recrystallized from methanol in a nitrogen atmosphere, dried in vacuo at 50 °C for 24 h, and stored under nitrogen in a refrigerator.

L-(+)-Lauroylcysteine methyl ester: mp 63.5–66.0 °C; TLC (1/1 hexanes/EtOAc) $R_f = 0.53$; $[\alpha]_D^{21} = +41.2 \pm 0.1^\circ$ ($c = 0.23$ g/mL, CHCl_3). Anal. Calcd: C, 60.53; H, 9.84. Found: C, 60.63; H, 9.66.

D-(–)-Lauroylcysteine methyl ester: same data as for the L-(+) isomer except $[\alpha]_D^{21} = -39.1 \pm 0.3^\circ$ ($c = 0.23$ g/mL, CHCl_3). Anal. Found: C, 60.77; H, 9.64.

DL-(±)-Lauroylcysteine methyl ester: same data as for the L-(+) isomer except mp 54.0–56.5 °C; $[\alpha]_D^{21}$, no rotation detected. Anal. Found: C, 60.62; H, 9.81.

Dilauroylcysteine Dimethyl Esters. L-Cystine (Sigma No. C 7755) and D-cystine (Sigma No. C 8505) were esterified as above for cysteine and reacted with 2 equiv of lauroyl chloride to yield the corresponding dilauroylcysteine dimethyl esters. The *meso*-cystine isomer was obtained by racemization of L-cystine, effected by refluxing in 20% HCl for 5 days,¹⁸ and subsequent fractional crystallization from the resulting mixture with D,L-cystine. An infrared spectrum (KBr pellet) obtained of the *meso*-cystine was identical to that found in the literature.¹⁹ It was then treated as above to obtain the *meso*-dilauroylcysteine dimethyl ester. The products were recrystallized repeatedly from distilled methanol and dried in vacuo at 50 °C for 24 h.

Attempts to synthesize D,L-dilauroylcysteine dimethyl ester using different sources of D,L-cystine (Sigma No. C 8630, Fluka No. 30220) resulted in crude products which did not recrystallize cleanly (more than one spot on the TLC plate). Thus, crystals of the D,L isomer were obtained by preparing a 1/1 mixture of the L- and D-dilauroylcysteine dimethyl esters, each in benzene solution. The benzene was removed, and the resulting product was allowed to crystallize from distilled methanol.

L-(+)-Dilauroylcysteine dimethyl ester: mp 97.4–98.5 °C; TLC (1/1 hexanes/EtOAc) $R_f = 0.30$; $[\alpha]_D^{21} = +78.2 \pm 2.4^\circ$ ($c = 0.92$ g/mL, CHCl_3). Anal. Calcd: C, 60.72; H, 9.56; N, 4.43; S, 10.13. Found: C, 60.85; H, 9.75; N, 4.50; S, 10.16.

D-(–)-Dilauroylcysteine dimethyl ester: same data as for the L-(+) isomer except $[\alpha]_D^{21} = -78.4 \pm 1.7^\circ$ ($c = 0.92$ g/mL, CHCl_3). Anal. Found: C, 60.62; H, 9.66; N, 4.44; S, 9.97.

DL-(±)-Dilauroylcysteine dimethyl ester was obtained from a 1/1 mixture of D and L isomers: mp 88.0–90.0 °C; $[\alpha]_D^{21}$, no rotation detected.

meso-Dilauroylcysteine dimethyl ester: mp 79.2–85.4 °C; TLC (1/1 hexanes/EtOAc) $R_f = 0.33$; $[\alpha]_D^{21}$, no rotation detected. Anal. Calcd: C, 60.72; H, 9.56; N, 4.43; S, 10.13. Found: C, 61.09; H, 9.84; N, 4.47; S, 9.81.

Stearoylthreonine Methyl Esters. L-Threonine methyl ester hydrochloride (Sigma No. T 5898, ~1 g) and DL-threonine methyl ester hydrochloride (Sigma No. T 8750, ~1 g) were each treated with 1 equiv

of stearoyl chloride as in the synthesis of stearoylcysteine methyl ester given above. D-Threonine (Sigma No. T 8250, ~500 mg) was esterified (see cysteine esterification above) before it was coupled to the acid chloride. The resulting stearoylthreonine methyl esters were recrystallized repeatedly from distilled methanol and dried in vacuo at 50 °C for 24 h.

L-*allo*-Threonine (Sigma No. T 2888, ~500 mg) and **D-*allo*-threonine** (Sigma No. T 3013, ~500 mg) were esterified and coupled to stearoyl chloride. Poor yields of the two crude *allo*-stearoylthreonine methyl ester products made repeated recrystallizations unfeasible. Thus, they were purified by preparative-scale TLC (Silica gel, 20 × 20 cm, Sigma No. T-6270) using a 15/1 $\text{CHCl}_3/\text{MeOH}$ mixture. The region corresponding to the pure product was scraped off and extracted from the silica gel using 1/1 $\text{CHCl}_3/\text{MeOH}$. This product was allowed to crystallize from distilled methanol. DL-*allo*-stearoylthreonine methyl ester crystals were obtained by mixture of the D-*allo* and L-*allo* crystals in 9/1 hexanes/EtOH, followed by solvent removal, in a manner similar to the procedure described above for DL-dilauroylcysteine dimethyl ester. The resulting solid racemate was allowed to crystallize from distilled methanol.

L-(–)-Stearoylthreonine methyl ester: mp 96.2–96.8 °C; TLC (15/1 $\text{CHCl}_3/\text{MeOH}$) $R_f = 0.29$; $[\alpha]_D^{21} = -1.0 \pm 0.1^\circ$ ($c = 1.00$ g/mL, CHCl_3). Anal. Calcd: C, 69.13; H, 11.35; N, 3.51. Found: C, 69.27; H, 11.14; N, 3.53.

D-(+)-Stearoylthreonine methyl ester: same data as the L-(–) isomer except $[\alpha]_D^{21} = +0.9 \pm 0.2^\circ$ ($c = 1.00$ g/mL, CHCl_3). Anal. Found: C, 69.39; H, 11.18; N, 3.57.

DL-(±)-Stearoylthreonine methyl ester: same data as the L-(–) isomer except mp 82.0–83.0 °C; $[\alpha]_D^{21}$, no rotation detected. Anal. Found: C, 69.25; H, 11.12; N, 3.47.

L-(–)-*allo*-Stearoylthreonine methyl ester: mp 101.8–102.8 °C; TLC (15/1 $\text{CHCl}_3/\text{MeOH}$) $R_f = 0.31$; $[\alpha]_D^{21} = -1.30 \pm 0.2^\circ$ ($c = 1.00$ g/mL, CHCl_3). Anal. Calcd: C, 69.13; H, 11.35; N, 3.51. Found: C, 70.16; H, 10.79; N, 2.49.

D-(+)-*allo*-Stearoylthreonine methyl ester: same data as the L-(–) isomer except $[\alpha]_D^{21} = +1.26 \pm 0.3^\circ$ ($c = 1.00$ g/mL, CHCl_3). Anal. Found: C, 69.20; H, 11.08; N, 3.55.

DL-(±)-*allo*-Stearoylthreonine methyl ester was obtained from a 1/1 mixture of D and L isomers: mp 87.5–89.0 °C; $[\alpha]_D^{21}$, no rotation detected.

Preparation of Crystals for Melting Point Diagrams. Crystals of a given D/L ratio were prepared by first weighing out accurate amounts of each enantiomer (~4–5 mg) to the nearest 0.001 mg on a Cahn RG electrobalance and then dissolving each into either purified 9/1 hexanes/EtOH or purified benzene in hand-calibrated 25-mL volumetric flasks. Amounts of each solution were delivered in the appropriate ratio by an Agla micrometer syringe into a 5-mL flask. The resulting mixed solutions were allowed to stand for 1 h, and the solvent was rotary evaporated. The isolated powder was allowed to crystallize from distilled methanol and then dried in vacuo at 50 °C for 24 h.

Monolayer Techniques. Langmuir Film Balance Techniques. The design and technical specifications of the Langmuir film balance used in our laboratory have been presented elsewhere.²⁰ It is sensitive to ± 0.005 dyn/cm film pressure.

The film balance was housed in a Puffer-Hubbard Uni-Therm cabinet during use, which both shields the balance from outside contamination and provides a controllable temperature environment. The temperature of the water in the film balance is controlled further by a glass serpentine coil placed in the trough, through which water is circulated from a Fisher constant-temperature bath. In order to reduce the evaporation of subphase (which affects surface temperature), the humidity in the cabinet is kept high by placing dishes of water inside.

After assembly of the film balance for an experiment, the subphase water was checked for cleanliness before spreading the film by moving the barrier from the end of the trough up to the floating barrier to make sure no buildup of surface pressure from surface contaminants had occurred. The overall performance of the system was checked daily by reproducing the well-known stearic acid monolayer isotherm²¹ using stearic acid purified especially for this project.⁷

The moving barrier was set at a position corresponding to an exposed area of $5.28 \times 10^{18} \text{ \AA}^2$. The surfactant was spread onto the surface so as to provide 4.403×10^{16} molecules to give a starting surface area of $120 \text{ \AA}^2/\text{molecule}$, at which value the surfactants of this study show no detectable surface pressure.

After 10–15 min were allowed for the evaporation of spreading solvent, the film was compressed by displacement of the moving barrier toward the floating barrier using the motor-driven wormscrew drive. When the

(16) Vogel, A. I. *A Textbook of Practical Organic Chemistry*, 3rd ed.; Longmans, Green and Co.: London, 1957; p 166.

(17) Zeelen, F. J.; Havinga, E. *Recl. Trav. Chim. Pays-Bas* 1958, 77, 267.

(18) Loring, H. S.; Du Vigneaud, V. *J. Biol. Chem.* 1933, 102, 287.

(19) Greenstein, J. P.; Winitz, M. *Chemistry of the Amino Acids*; John Wiley & Sons: New York, 1961; Vol. 3, p 1925.

(20) Thompson, O. Ph.D. Dissertation, University of Pittsburgh, Pittsburgh, PA, 1981.

(21) Reference 5, p 220.

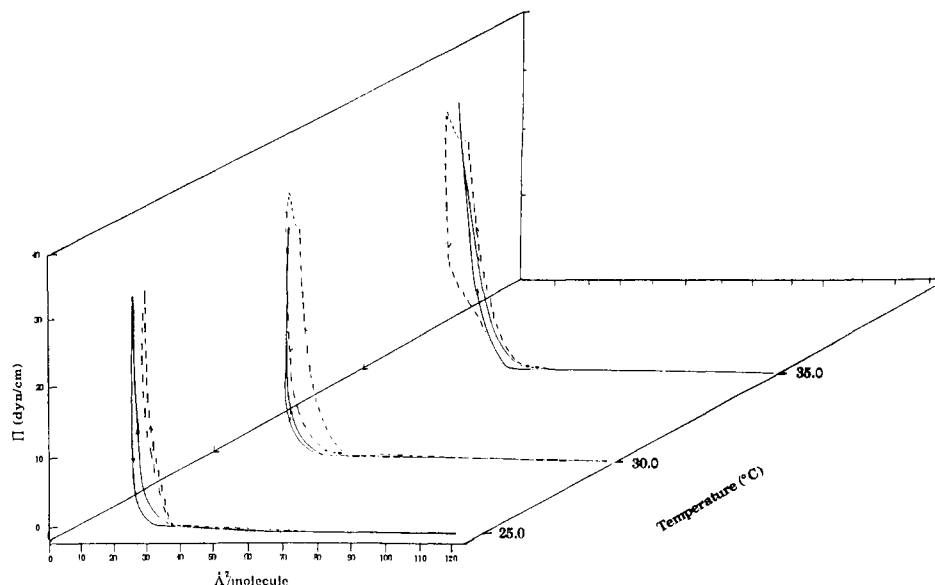


Figure 2. Surface pressure vs area isotherms for compression and expansion of enantiomeric (---) and racemic (—) stearylcytosteine methyl esters (SCME) on an aqueous subphase at various temperatures.

accumulated surface pressure reached 40 dyn/cm, the motor was reversed and the film expanded back to zero surface pressure. The film was then removed by aspiration.

The stability limits of monolayer films were checked by halting the compression of the film at various points and monitoring the rate of surface pressure loss over time (typically 2 min). Films were judged "stable" if the loss rate was less than 0.1 dyn/cm/min.

Surface Viscometry. The instrument used was designed originally as a Verger "zero-order" film balance²² to measure enzyme kinetics of phospholipid films, but was adapted by Dr. Philip Rose in this laboratory to become a canal surface viscometer. It was housed in an aluminum cabinet during use. The technical specifications of this instrument and also the details of its use have been presented previously.¹²

The film is forced through a narrow canal by a moving barrier which is displaced as needed by a feedback mechanism so as to maintain constant film pressure. Displacement of the barrier is monitored by a strip chart recorder over a 5-min period. From the slope of the linear plot of displacement versus time and the known width of the trough, one can calculate the rate at which the film moves through the canal in cm²/s. This value is used in the Harkins-Kirkwood equation²³ (eq III-3) to determine the coefficient of surface shear viscosity, η_s , for a canal whose length is significantly greater than its width.

$$\eta_s = (\Pi_2 - \Pi_1)w^3/12QL \quad (\text{III-3})$$

Here, $(\Pi_2 - \Pi_1)$ = the difference in surface pressure (dyn/cm) between that on the film in the pressurized compartment and that in the compartment into which the film flows, while w = canal width (cm), Q = rate of film flow (cm²/s), and L = canal length (cm). The classical correction ($w\eta_0/\pi$) for vicinal drag²³ of the subphase is omitted in these viscosity calculations, since we are interested primarily in differential viscosities as a function of stereochemistry.

Differential Scanning Calorimetry of Surfactant Crystals. Thermograms of surfactant crystals were acquired on a Perkin-Elmer DSC 7 instrument, which was calibrated using an indium standard. Samples of 1–3 mg were weighed on an analytical balance and sealed in aluminum pans. These samples were placed in the instrument and equilibrated thermally at the starting temperature of 30 °C. Heating thermograms were recorded in the 30–150 °C range and at scan rates of 5 and 10 °C/min. The calculation of transition enthalpies was performed directly by Perkin-Elmer software through a personal computer interfaced to the DSC apparatus.

Data Analysis. The data presented here are based on several replications of each experiment and are analyzed at the 95% confidence limit using "t" values for that particular confidence interval.²⁴ Errors in the thermodynamic properties of spreading (ESPs) were propagated from estimated standard deviations of the contributing measured values in the usual manner.²⁵

Each surface pressure vs area isotherm reported here was reproduced 5–10 times, each time from a freshly spread film. The measured areas generally agreed to within $\pm 2 \text{ \AA}^2/\text{molecule}$, and the corresponding surface pressures agreed to within $\pm 0.3 \text{ dyn/cm}$. Isotherms were recorded on strip charts as well as digitally on a personal computer, where they were stored and manipulated on floppy disks.

Equilibrium spreading pressures are the average of 3–5 replications, starting each time with fresh crystals and subphase. Viscosity values are the average of 5–7 replications for each surface pressure studied, starting each time with a fresh film.

The heats and entropies of fusion, obtained from the DSC thermograms, are an average of three replications, using fresh crystals for each run.

Results

In this section, the results from the "two-dimensional" monolayer experiments are presented along with studies of the phase behavior involving the three-dimensional crystals of each surfactant. In this way, the phase behavior in the two types of systems can be compared directly as a function of stereochemistry. Some data from our previous study of SSME⁹ will be repeated for direct comparison with SCME and STME.

Surface Pressure vs Area Isotherms. Figure 2 shows the compression/expansion Π/A isotherms for enantiomeric and racemic SCME on pure water at 25.0, 30.0, and 35.0 °C, cycled at a rate of $19.24 \text{ \AA}^2/\text{molecule}/\text{min}$ and spread from solution in purified 9/1 hexanes/EtOH. The racemic film is slightly more condensed than the enantiomeric film at all temperatures and displays a smaller degree of hysteresis (difference between the compression and expansion cycles) at 30 and 35 °C. No changes were observed in the isotherms when the films were cycled at rates of 7.71 and $29.80 \text{ \AA}^2/\text{molecule}/\text{min}$.

Figure 3 gives the isotherms for enantiomeric (i.e., *R,R* or *S,S*) and racemic DLCDME spread from solution in benzene on pure water at 20.0, 25.0, 30.0, and 35.0 °C. The racemic film has a collapse pressure that is much lower than that of the enantiomeric film at all temperatures studied.

At surface pressures below the collapse point of either film, the isotherms for enantiomeric and racemic DLCDME are identical within experimental error, and they show no hysteresis if the films are expanded before the collapse pressure is reached. A full set of isotherms was prepared for the meso isomer, but since they are nearly superimposable on those for the enantiomers at the same temperature, we have not reproduced them here.

Figure 4 gives the compression/expansion Π/A isotherms for STME on pure water at 15.5, 20.0, 25.0, 30.0, and 35.0 °C. The

(22) Verger, R.; de Haas, G. H. *Chem. Phys. Lipids* **1973**, *10*, 127.

(23) Harkins, W. D.; Kirkwood, J. G. *J. Chem. Phys.* **1938**, *6*, 298.

(24) Skoog, D. A. *Principles of Instrumental Analysis*, 3rd ed.; Saunders College Publishing: Philadelphia, 1985; p 11.

(25) Swokowski, E. W. *Calculus with Analytical Geometry*, 2nd ed.; Prindle, Weber, and Schmidt: Boston, 1979; p 768.

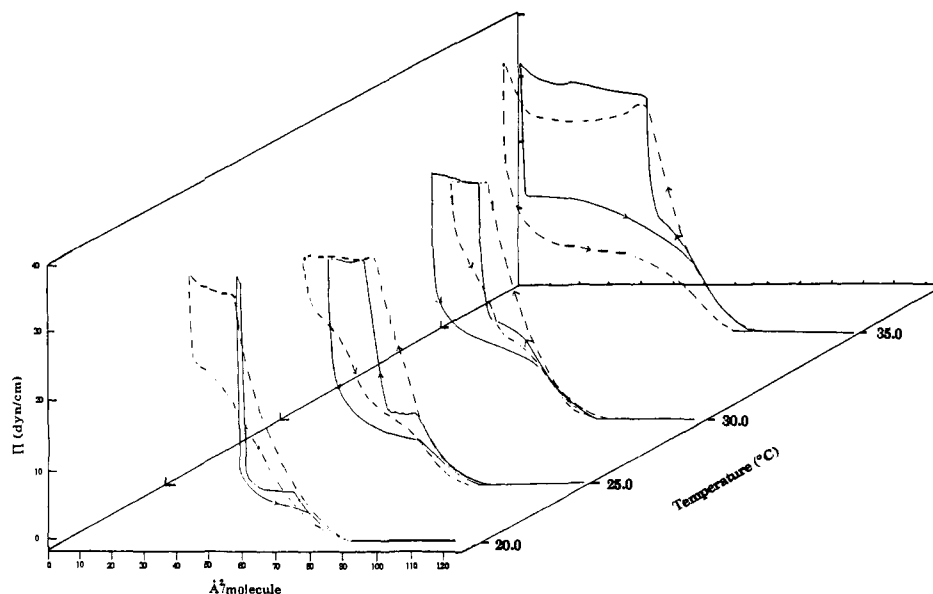


Figure 3. Surface pressure vs area isotherms for compression and expansion of enantiomeric (---) and racemic (—) diluroylcystine dimethyl esters (DLCDME) on an aqueous subphase at various temperatures.

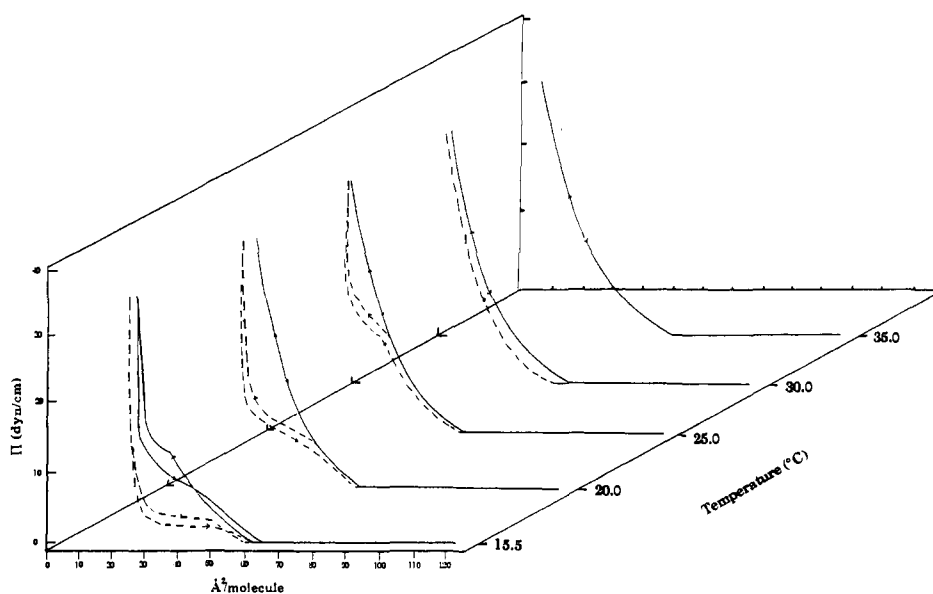


Figure 4. Surface pressure vs area isotherms for compression and expansion of enantiomeric (---) and racemic (—) stearylthreonine methyl esters (STME) on an aqueous subphase at various temperatures.

films were spread from solution in 9/1 hexanes/EtOH, and the isotherms shown were cycled at a rate of $19.24 \text{ \AA}^2/\text{molecule}/\text{min}$. Films cycled at other rates (7.71 and $29.80 \text{ \AA}^2/\text{molecule}/\text{min}$) yielded the same isothermal curves.

It is apparent from these isotherms that, as usual, the chiral recognition decreases strongly with increasing temperature. The main difference between the enantiomeric and racemic films of STME is related to phase behavior involving the so-called "liquid-expanded" and "liquid-condensed" monolayer states, which is treated in more detail below.

Hysteresis is only observed in films for which a phase-transition "kink" occurs during the compression of the film. For those films that remain in an expanded state throughout the compression of the monolayer (up to 40 dyn/cm), the expansion isotherm follows the same path as the compression isotherm. Also, for the films that have a transition point, isotherms show no hysteresis if expanded before the transition point is reached.

The isotherms of the allo isomer are so similar to those of the enantiomers of STME¹⁵ that they are not reproduced here.

Figure 5 presents data for SSME from ref 9. These curves should be compared with those of SCME, which carries a thiol group instead of a hydroxyl, and with STME, which bears a

methyl group on the same carbon as the hydroxyl. Striking differences are clear.

Phase Behavior of STME Monolayers as a Function of Temperature. As noted above, the phase behavior of the STME films (and their allo diastereomers) involves a transition from the liquid-expanded monolayer state to the liquid-condensed monolayer state. Historically, the surface pressures at which this type of transition takes place have been found to vary linearly with temperature.²⁶ The transition pressures of the STME films vs temperature, taken from the corresponding Π/A isotherms for each temperature, are plotted in Figure 6. The narrow temperature range of the plots is a result of the fact that the films reach a critical temperature within the range of monolayer study ($15\text{--}35 \text{ }^\circ\text{C}$), a temperature above which the films do not show a transition (up to 40 dyn/cm) regardless of surface pressure. This critical temperature is $\sim 20 \text{ }^\circ\text{C}$ for the racemic films and $\sim 30 \text{ }^\circ\text{C}$ for the enantiomeric films.

The plots indicate that these films have a linear correlation between Π^{trans} and temperature. The slopes ($d\Pi^{\text{trans}}/dT$) and

(26) Kellner, B. M.; Müller-Landau, F.; Cadenhead, D. A. *J. Colloid Interface Sci.* **1978**, *66*, 597.

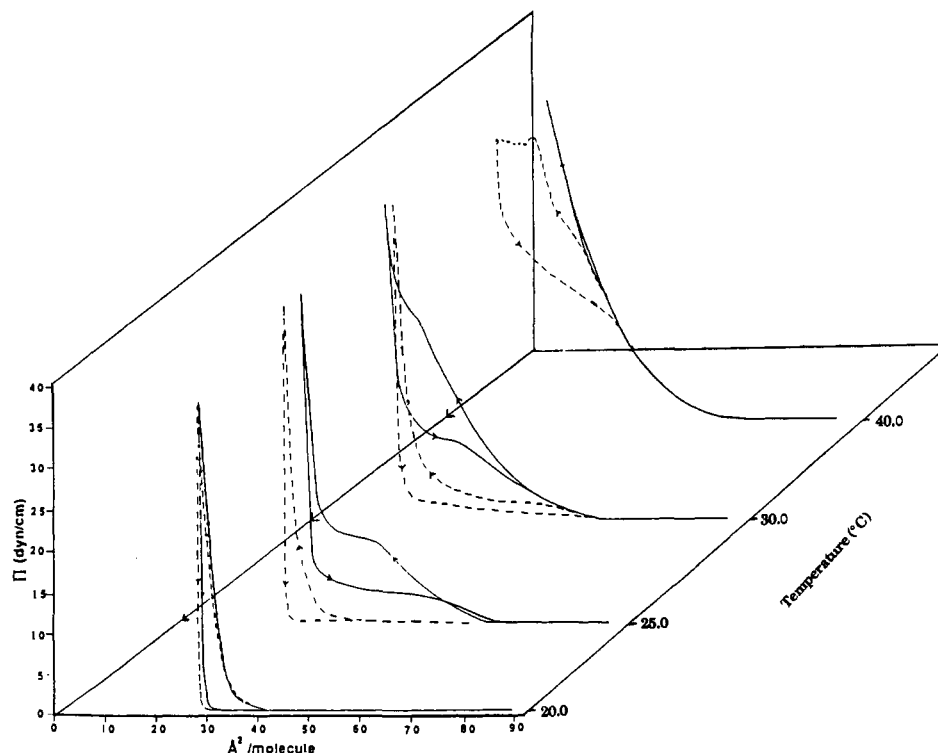


Figure 5. Surface pressure vs area isotherms for compression and expansion of enantiomeric (---) and racemic (—) stearoylserine methyl esters (SSME) on an aqueous subphase at various temperatures. Data from refs 9 and 28.

Table I. Characteristics of Transition Pressure vs Temperature Plots for Monolayers of Stearoylthreonine Methyl Esters (STME) and *allo*-Stearoylthreonine Methyl Esters (*allo*-STME)

	$d(\Pi^{\text{trans}})/dT$ (dyn/cm/°C)	T_0 (°C)
enantiomeric STME	1.2 ± 0.1	13.8 ± 0.8
racemic STME	3.5 ± 0.4	12.3 ± 0.1
enantiomeric <i>allo</i> -STME	1.7 ± 0.2	14.5 ± 0.7
racemic <i>allo</i> -STME	1.9 ± 0.1	12.7 ± 0.3

γ -intercepts (T_0) of these plots are given in Table I. The slope indicates the degree of expansion of the monolayer with increasing temperature, while the T_0 value indicates the temperature at which the liquid-expanded phase first appears. There is almost no variation of T_0 as a function of stereochemistry for these films, as they each give a value near 12–14 °C. The rates of expansion above this range, however, do depend on stereochemistry. The racemic STME film has a slope that is 3 times that of its enantiomeric form. Plots for the *allo*-STME films are also linear and differ only slightly from those in Figure 6, as shown in Table I.

Thermodynamics of Spreading. The surface free energies, entropies, and enthalpies of spreading for enantiomeric, racemic, and *meso*-DLCDME, given in Table II, were derived from the following relationships:²⁷

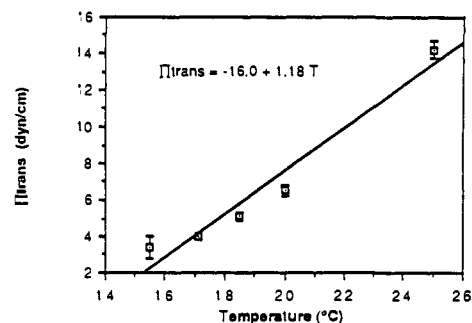
$$\Delta G_s^\circ = -A^\circ \Pi^\circ \quad (1)$$

$$\Delta S_s^\circ = A^\circ (d\Pi^\circ/dT) \quad (2)$$

$$\Delta H_s^\circ = T A^\circ (d\Pi^\circ/dT) - A^\circ \Pi^\circ \quad (3)$$

where A° is the average area per molecule of the spread film, taken directly from the Π/A isotherm at the equilibrium spreading pressure, Π° . These thermodynamic properties were measured at 20.0, 25.0, 30.0, and 35.0 °C. The racemic crystals spread spontaneously only at 35.0 °C. The *meso* crystals showed the greatest propensity to spread, displaying the largest values for all

a) Enantiomeric



b) Racemic

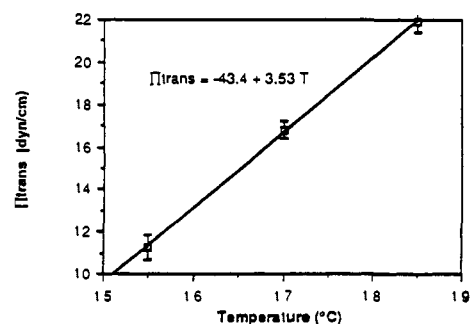


Figure 6. Transition pressure (Π^{trans}) vs temperature for monolayers of (a) enantiomeric and (b) racemic stearoylthreonine methyl ester.

quantities measured at all temperatures.

The equilibrium spreading pressures and surface free energies, entropies, and enthalpies of spreading for racemic STME and enantiomeric and racemic *allo*-STME are given in Table III. Enantiomeric STME crystals do not spread (up to 48 h) at any of the temperatures studied. The other isomeric forms spread only at temperatures above 20 °C.

Stability Limits. The maximum surface pressure at which the films were stable was measured according to the procedure de-

(27) Harkins, W. D.; Young, T. F.; Boyd, E. J. *J. Chem. Phys.* 1940, 8, 954.

Table II. Equilibrium Spreading Pressures and Surface Excess Free Energies, Entropies, and Enthalpies of Spreading for Enantiomeric, Racemic, and Meso Dilauroylcystine Dimethyl Esters

temp (K)	Π^c (dyn/cm)			A^c ($\text{\AA}^2/\text{molecule}$)			ΔG_s° (cal/mol)		
	enan	rac	meso	enan	rac	meso	enan	rac	meso
293	<i>a</i>	<i>a</i>	4.82 ± 1.04	<i>a</i>	<i>a</i>	79.8 ± 1.2	<i>a</i>	<i>a</i>	-554 ± 89
298	0.70 ± 0.20	<i>a</i>	7.85 ± 1.17	86.9 ± 1.0	<i>a</i>	76.7 ± 0.3	-88 ± 18	<i>a</i>	-867 ± 92
303	3.19 ± 0.42	<i>a</i>	10.16 ± 1.67	84.6 ± 2.2	<i>a</i>	73.6 ± 1.1	-388 ± 43	<i>a</i>	-1080 ± 130
308	4.04 ± 0.37	0.29 ± 0.19	11.71 ± 0.37	81.8 ± 2.7	93.4 ± 1.2	73.6 ± 1.8	-476 ± 41	-39 ± 18	-1240 ± 48

temp (K)	ΔS_s° (cal/mol/deg)			ΔH_s° (kcal/mol)		
	enan	rac	meso	enan	rac	meso
293	<i>a</i>	<i>a</i>	52.8 ± 1.7	<i>a</i>	<i>a</i>	14.9 ± 0.6
298	41.8 ± 1.4	<i>a</i>	50.8 ± 0.4	12.4 ± 0.4	<i>a</i>	14.2 ± 0.2
303	40.7 ± 3.2	<i>a</i>	48.7 ± 1.6	11.9 ± 1.0	<i>a</i>	13.7 ± 0.6
308	39.3 ± 3.9		48.7 ± 2.6	11.6 ± 1.3		13.8 ± 0.8

^aNo film spreading detected at this temperature.

Table III. Equilibrium Spreading Pressures and Surface Excess Free Energies, Entropies, and Enthalpies of Spreading for Racemic Stearoylthreonine Methyl Ester (rac) and Enantiomeric and Racemic *allo*-Stearoylthreonine Methyl Esters (enan-*allo* and rac-*allo*)^{a,b}

temp (K)	Π^c (dyn/cm)			A^c ($\text{\AA}^2/\text{molecule}$)			ΔG_s° (cal/mol)		
	rac	enan- <i>allo</i>	rac- <i>allo</i>	rac	enan- <i>allo</i>	rac- <i>allo</i>	rac	enan- <i>allo</i>	rac- <i>allo</i>
298	0.98 ± 0.34	<i>c</i>	3.58 ± 0.23	60.5 ± 1.5	<i>c</i>	56.4 ± 1.0	-85 ± 32	<i>c</i>	-129 ± 24
303	2.67 ± 0.30	1.17 ± 0.90	3.99 ± 0.69	60.4 ± 1.2	59.7 ± 1.5	56.0 ± 1.4	-232 ± 31	-101 ± 79	-322 ± 64
303		(0.5 ± 0.2)	(4.2 ± 0.3)		(64 ± 3)	(54 ± 2)		(-50 ± 20)	(-330 ± 30)
308	3.90 ± 0.30	3.51 ± 0.35	4.64 ± 0.28	56.7 ± 1.1	54.2 ± 1.6	54.3 ± 1.2	-318 ± 31	-274 ± 35	-363 ± 30

temp (K)	ΔS_s° (cal/mol/deg)			ΔH_s° (kcal/mol)		
	rac	enan- <i>allo</i>	rac- <i>allo</i>	rac	enan- <i>allo</i>	rac- <i>allo</i>
298	25.4 ± 6.2	<i>c</i>	8.6 ± 1.3	7.5 ± 1.9	<i>c</i>	2.3 ± 1.3
298		(44 ± 4)	(47 ± 4)			
303	25.4 ± 6.1	40.2 ± 22	8.6 ± 4.3	7.5 ± 1.9	12.1 ± 6.7	2.3 ± 1.4
303					(13.3 ± 1.2)	(14.3 ± 1.2)
308	23.8 ± 5.7	36.5 ± 21	8.3 ± 4.2	7.0 ± 1.8	11.0 ± 6.5	2.2 ± 1.3

^aEnantiomeric STME does not spread at any of these temperatures ($\Pi^c = 0$). ^bNo film spreading detected at this temperature. ^cNumbers in parenthesis are for SSME at same temperature.⁹

scribed in the Experimental Section; values are reported in Table IV. Both the enantiomeric and racemic films of SCME were unstable at all surface pressures at 25 and 30 °C. At 35 °C, the films were only stable at pressures of less than 1 dyn/cm.

The enantiomeric film of DLCDME tends to be stable to higher surface pressures than the racemic one. The stability limits for the racemic film are within 1 dyn/cm of the corresponding collapse pressures at each temperature.

Surface Shear Viscosities. The viscosities of the DLCDME monolayers at 20.0, 25.0, and 30.0 °C are given in Table V for enantiomeric, racemic, and meso films at surface pressures of 5.0, 12.5, and 20.0 dyn/cm. The results shown are for a canal width of 1.5 mm. Runs were done for films using canal widths of 1.0 and 2.0 mm as well, and the calculated viscosity values for these other widths were within experimental error of those reported here. Thus, all of the films display "Newtonian" behavior since their measured viscosities are independent of shear rate (which can be changed effectively by varying canal width).

Viscosity values for DLCDME are generally independent of stereochemistry at each temperature and surface pressure studied. The viscosities of the enantiomeric and racemic STME and *allo*-STME monolayers are given using the same conditions as for the measurement of DLCDME viscosities. The threonine surfactant films all exhibited Newtonian behavior. The viscosity values are generally independent of stereochemistry at each temperature and surface pressure except in cases where some films are in the liquid-condensed state. In those cases, the viscosities are ~2–3 times higher than the films in the liquid-expanded state.

Crystals. Only small differences were noted in the solid-state IR spectra of enantiomeric and racemic SCME. However, their melting points differed by more than 20 °C (enantiomeric mp 86.2–87.0 °C; racemic mp 64.5–65.5 °C). Their melting behavior

Table IV. Monolayer Stability Limits for Spread Films of Amino Acid Surfactants on a Pure Water Subphase

temp (°C)	stability limits (dyn/cm)		
	enan	rac	meso
	Dilauroylcystine Dimethyl Esters		
20.0	~7	~7	~8
25.0	~10	~9	~9
30.0	~12	~11	~17
35.0	~19	~12	~28
	Stearoylthreonine Methyl Esters		
15.5	~3	~10	
20.0	~6	~19	
25.0	~11	~30	
30.0	~21	~30	
35.0	~20	~20	
	<i>allo</i> -Stearoylthreonine Methyl Esters		
15.5	~2	~4	
20.0	~8	~13	
25.0	~16	~29	
30.0	~18	~30	
35.0	~25	~18	
	Stearoylserine Methyl Ester ⁹		
20.0	unstable at all Π	unstable at all Π	
25.0	unstable at all Π	~2.5	
30.0	~0.5	~15	
35.0	~19	~21	

was investigated further by DSC; the calculated enthalpies and entropies of fusion are presented in Table VI. The calculated energies of fusion indicate that the racemic crystals have slightly higher values for both enthalpy and entropy of fusion.

Table V. Surface Shear Viscosities for Monolayers of Amino Acid Surfactants at Surface Pressures (Π) of 5.0, 12.5, and 20.0 dyn/cm and Temperatures of 20, 25, and 30 °C on a Pure Water Subphase^a

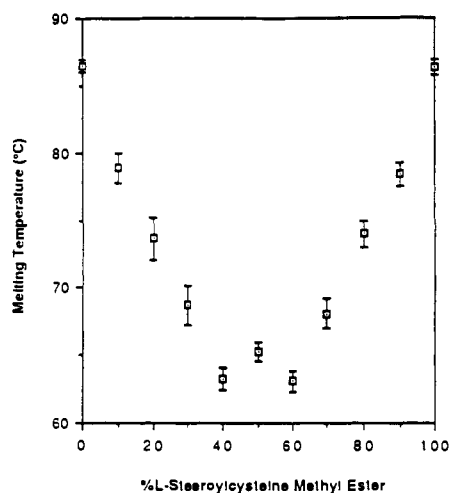
film	surface shear viscosity (surface mP)								
	20 °C			25 °C			30 °C		
	$\Pi = 5.0$	$\Pi = 12.5$	$\Pi = 20.0$	$\Pi = 5.0$	$\Pi = 12.5$	$\Pi = 20.0$	$\Pi = 5.0$	$\Pi = 12.5$	$\Pi = 20.0$
Dilauroylcystine Dimethyl Esters									
enan	0.85 ± 0.09	0.92 ± 0.08	0.58 ± 0.03	0.75 ± 0.05	0.81 ± 0.05	0.58 ± 0.03	0.88 ± 0.09	0.91 ± 0.09	0.62 ± 0.07
rac	0.85 ± 0.08	<i>b</i>	<i>b</i>	0.73 ± 0.11	<i>b</i>	<i>b</i>	0.78 ± 0.08	<i>b</i>	<i>b</i>
meso	0.91 ± 0.09	0.87 ± 0.06	0.54 ± 0.04	0.65 ± 0.05	0.72 ± 0.03	0.49 ± 0.06	0.78 ± 0.06	0.83 ± 0.10	0.62 ± 0.05
Stearoylthreonine Methyl Esters									
enan	0.91 ± 0.03	2.14 ± 0.21	3.27 ± 0.28	1.17 ± 0.07	0.84 ± 0.11	2.96 ± 0.29	0.34 ± 0.04	0.37 ± 0.01	0.40 ± 0.04
rac	0.90 ± 0.11	0.87 ± 0.14	1.14 ± 0.09	1.15 ± 0.09	0.99 ± 0.13	1.23 ± 0.11	0.38 ± 0.02 (0.535 ± 0.040)	0.33 ± 0.01	0.38 ± 0.01
enan-allo	0.98 ± 0.07	1.93 ± 0.08	3.25 ± 0.23	1.21 ± 0.11	0.75 ± 0.04	1.12 ± 0.06	0.36 ± 0.03 (0.666 ± 0.109)	0.35 ± 0.03	0.43 ± 0.04
rac-allo	0.86 ± 0.09	1.14 ± 0.09	1.47 ± 0.22	1.20 ± 0.22	0.76 ± 0.06	0.90 ± 0.06	0.46 ± 0.07	0.52 ± 0.04	0.63 ± 0.06

^aNumbers in parentheses are for SSME. ^bFilm is above collapse pressure.

Table VI. Heats and Entropies of Fusion for Stearoylcysteine Methyl Ester (SCME), Dilauroylcystine Dimethyl Ester (DLCDME), Stearoylthreonine Methyl Esters (STME and *allo*-STME), and Stearoylserine Methyl Ester (SSME)^a

	transition temp (K)	ΔH_f° (kcal/mol)	ΔS_f° ^a (cal/mol/K)
enan SCME	359.8	12.5 ± 1.5	34.7 ± 4.1
rac SCME	338.2	15.1 ± 0.2	44.6 ± 0.5
enan DLCDME	368.5	13.8 ± 0.1	37.4 ± 0.3
rac DLCDME	358.4	17.1 ± 0.2	47.7 ± 0.6
meso DLCDME	357.3	18.2 ± 0.4	50.9 ± 1.1
enan STME	369.7	18.5 ± 0.2	50.0 ± 0.4
rac STME	355.7	14.8 ± 0.6	41.6 ± 1.6
enan <i>allo</i> -STME	375.5	14.5 ± 0.5	38.6 ± 1.2
rac <i>allo</i> -STME	361.4	15.1 ± 0.2	41.8 ± 0.5
enan SSME	362.1	23.0 ± 1.3	63.5 ± 4.0
rac SSME	367.2	16.4 ± 1.5	45.0 ± 4.1

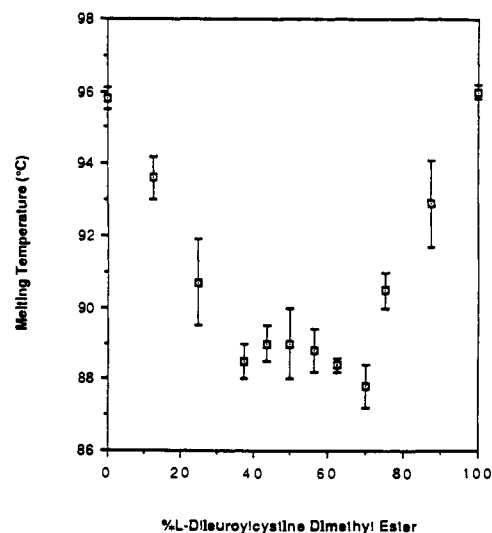
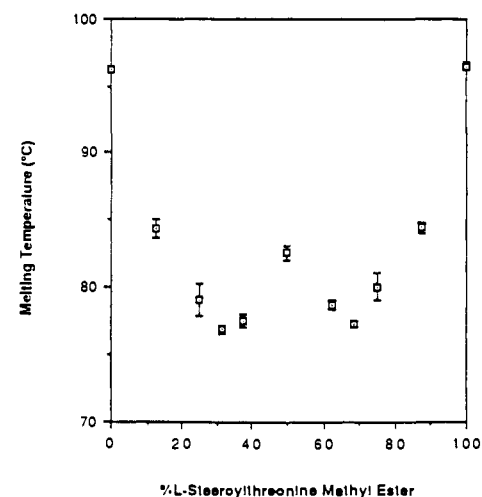
^a $\Delta S_f^\circ = \Delta H_f^\circ / T_{trans}$.

**Figure 7.** Melting point vs composition phase diagram for stearyl-cysteine methyl ester.

A melting point diagram of SCME (Figure 7) with carefully mixed crystals of the antipodes indicates racemic compound formation at the 50/50 mixture.

The crystals of SCME did not spread ($ESP = 0$) on a pure water subphase at any temperature at which the monolayers were studied, even on runs of up to 48 hours, so comparison with the surface behavior of mixtures of the enantiomers could not be made.

The solid-state IR spectra of enantiomeric and racemic DLCDME crystals were practically identical. The enantiomeric crystals melted at 97.4–98.5 °C, while the racemic crystals melted in the range 88–90.0 °C. The DSC thermograms of enantiomeric, racemic, and *meso*-DLCDME provide thermodynamic properties for fusion in Table VI.

**Figure 8.** Melting point vs composition phase diagram for dilauroyl-cystine methyl ester.**Figure 9.** Melting point vs composition phase diagram for stearyl-threonine methyl ester.

The melting behavior as a function of enantiomeric composition (Figure 8) suggested formation of a racemic compound especially in view of racemate formation for the other compounds of this series.

The IR spectrum of *meso*-DLCDME was similar for the enantiomeric and racemic crystals. The melting range of the *meso* crystals (79.2–85.4 °C) was somewhat broader, however.

The IR spectrum of racemic STME has a broader OH stretch than the enantiomeric crystals, which show a rather sharp peak

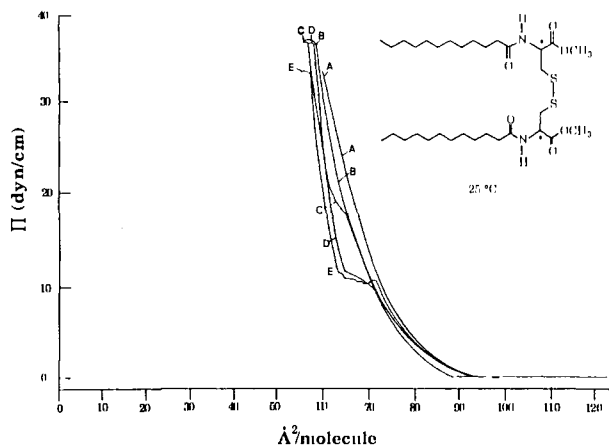


Figure 10. Surface pressure vs area isotherms for the compression of various enantiomeric mixtures of dilauroylcystine dimethyl esters on a pure water subphase at 25.0 °C. % L(or D) isomer: A = 100%; B = 87.5%; C = 75.0%; D = 62.5%; E = 50.0%.

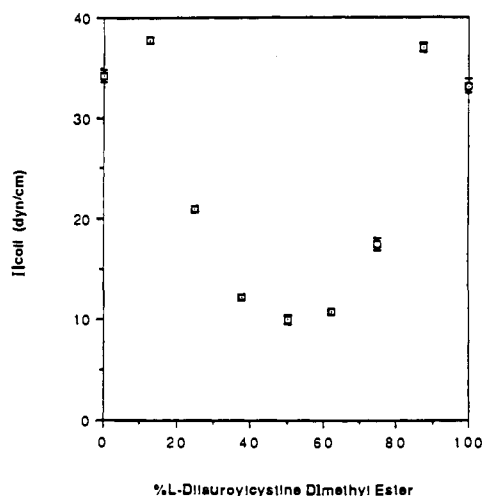


Figure 11. Collapse pressure (Π^{coll}) vs composition phase diagram for monolayers of dilauroylcystine dimethyl ester at 25.0 °C.

for this mode. Apart from this difference, the spectra are quite similar. The racemic crystals melt at 82.0–83.0 °C, while the enantiomers melt ~ 14 °C higher at 96.2–96.8 °C. The enantiomeric crystals have higher heats and entropies associated with the melting process than do the racemic crystals (Table VI). A melting point diagram for enantiomeric mixtures of STME is given in Figure 9. This plot implies racemic compound formation at the 50/50 mixture for STME crystals.

The IR spectra of the enantiomeric and racemic *allo*-STMEs were virtually identical and also were similar to those of the STME crystals, with the exception that the OH stretch for each of the *allo* spectra was broad and centered ~ 60 cm^{-1} below the values for STME crystals. The enantiomeric *allo*-STME crystals melted at 101.8–102.8 °C; the racemic crystals melted at 87.5–89.0 °C. The thermodynamics for fusion of the enantiomers of STME differs little from that of their *allo* isomer (Table VI).

Mixed Monolayers of Enantiomers. In order to provide “two-dimensional” analogues to the melting point curves of the crystals, isotherms were measured for mixtures of the enantiomers of DLCME and STME. Compression isotherms for DLCME mixtures, obtained at 25.0 °C, are shown in Figure 10. The compression rate was 19.24 $\text{\AA}^2/\text{molecule}/\text{min}$. The collapse pressures (Π^{coll}) of the films vs enantiomeric composition are plotted in Figure 11.

Compression isotherms for D and L mixtures of STME at 15.5 °C are shown in Figure 12. This temperature was chosen for study because all compositions at 15.5 °C show a transition point. This allows a complete plot of the transition pressure (Π^{trans}) vs enantiomeric composition to be constructed for these monolayer

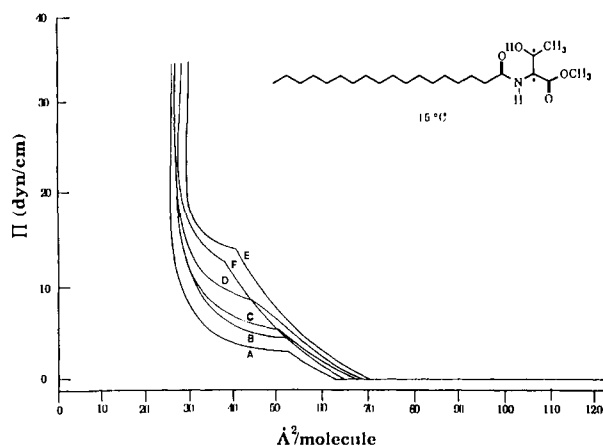


Figure 12. Surface pressure vs area isotherms for the compression of various enantiomeric mixtures of stearylthreonine methyl esters on a pure water subphase at 15.5 °C. % L(or D) isomer: A = 100%; B = 87.5%; C = 75.0%; D = 62.5%; E = 50.0%.

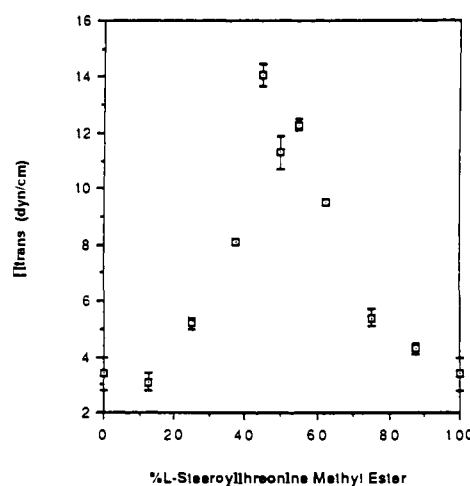


Figure 13. Transition pressure (Π^{trans}) vs composition phase diagram for monolayers of stearylthreonine methyl ester at 15.5 °C.

films, as shown in Figure 13. Transition pressures were measured by extrapolating the linear portions of the Π/A curve just below and above the transition point and taking the intersection of these lines as the Π^{trans} values.²⁶ The 100% L- or D-STME films give the lowest value for Π^{trans} ; however, there is a local minimum about the racemic (50%) composition.

Diastereomeric Molecular Recognition in Mixed Monolayers. The results involving diastereomeric monolayer mixtures show them to be one of two types: (1) mixtures of diastereomers of a single chiral surfactant and (2) mixtures of two different surfactants, each of which is chiral. Both types are treated below. First, the results of studies involving mixtures of diastereomeric L- and *meso*-DLCDME are presented, followed by results of studies of mixtures of L-STME with its D- and L-*allo* diastereomers.

Next, studies involving STME and SCME, each mixed with stearylserine methyl ester (SSME) are presented. SSME was chosen as a mixture component with STME and SCME for two reasons: (1) SSME is closely related structurally to both STME and SCME, which should increase the likelihood of truly mixed films; (2) SSME has shown considerable enantiomeric recognition properties in previous monolayer studies.^{9,28}

(1) Mixtures of a Single Chiral Surfactant. The compression Π/A isotherms for mixtures of L-DLCDME and *meso*-DLCDME at various ratios are given in Figure 14. These were obtained at 25 °C at a compression rate of 19.24 $\text{\AA}^2/\text{molecule}/\text{min}$. There

(28) Harvey, N. G. Ph.D. Dissertation, Duke University, Durham, NC, 1988.

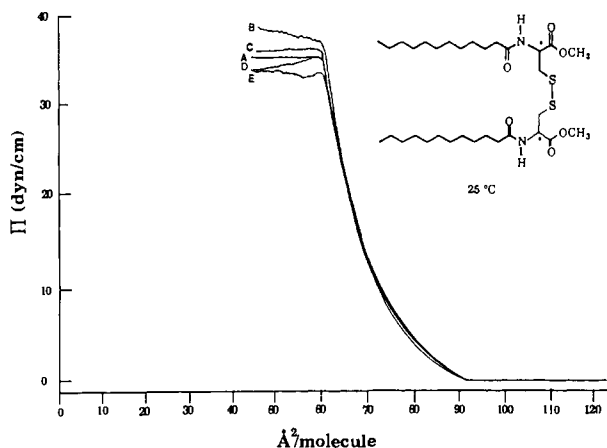


Figure 14. Surface pressure vs area isotherms for the compression of L- and *meso*-dilauroylcystine dimethyl esters and their mixtures on a pure water subphase at 25.0 °C. % L isomer: A = 0.0% (100.0% *meso*); B = 25.0%; C = 50.0%; D = 75.0%; E = 100.0% (0.0% *meso*).

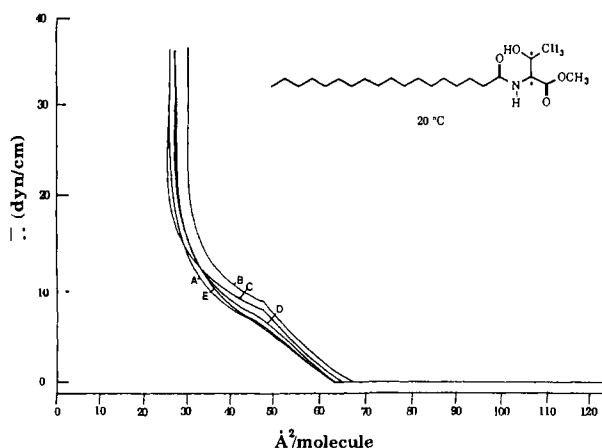


Figure 15. Surface pressure vs area isotherms for the compression of L-stearoylthreonine methyl ester, L-*allo*-stearoylthreonine methyl ester, and their mixtures on a pure water subphase at 20.0 °C. % L isomer: A = 100.0% (0.0% L-*allo*); B = 75.0%; C = 50.0%; D = 25.0%; E = 0.0% (100.0% L-*allo*).

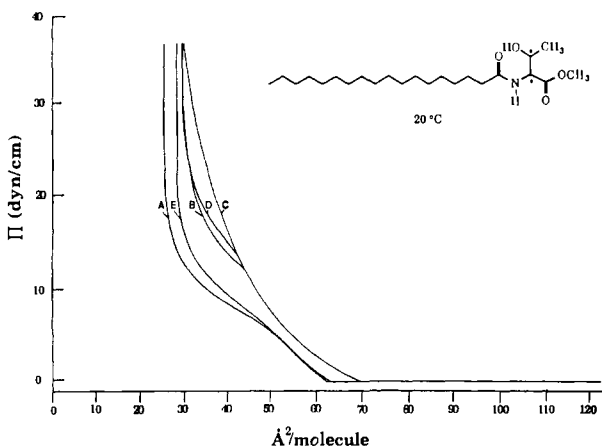


Figure 16. Surface pressure vs area isotherms for the compression of L-stearoylthreonine methyl ester, D-*allo*-stearoylthreonine methyl ester, and their mixtures on a pure water subphase at 20.0 °C. % L isomer: A = 100.0% (0.0% D-*allo*); B = 75.0%; C = 50.0%; D = 25.0%; E = 0.0% (100% D-*allo*).

is little difference in the curves as a function of composition, although the collapse behavior is somewhat different for each isotherm. Identical results were obtained for mixtures of D-DLCDME and *meso*-DLCDME.

Figures 15 and 16 give the compression Π/A isotherms for mixtures of L-STME + L-*allo*-STME and L-STME + D-*allo*-

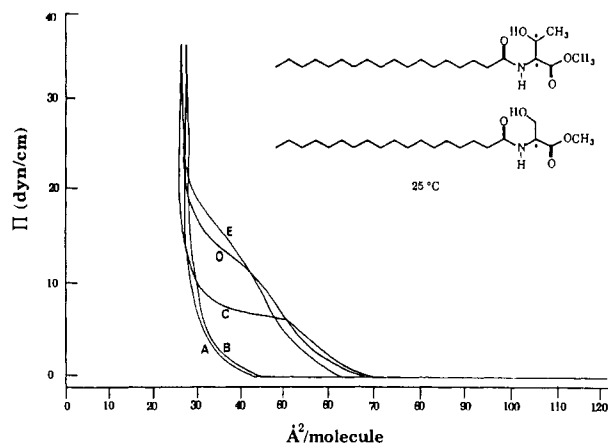


Figure 17. Surface pressure vs area isotherms for the compression of L-stearoylthreonine methyl ester (L-STME), L-stearoylserine methyl ester (L-SSME), and their mixtures on a pure water subphase at 25.0 °C. % L-STME: A = 0.0% (100.0% L-SSME); B = 25.0%; C = 50.0%; D = 75.0%; E = 100.0% (0.0% L-SSME).

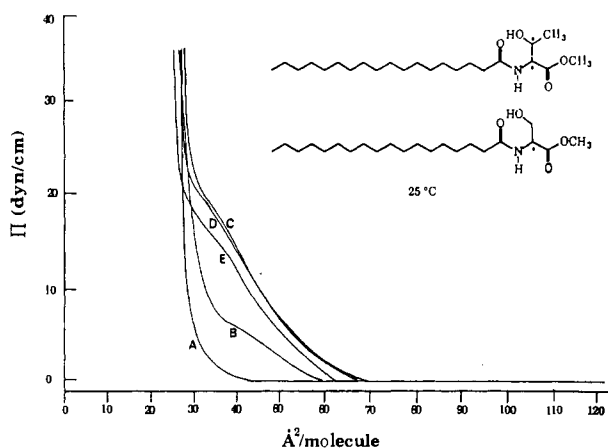


Figure 18. Surface pressure vs area isotherms for the compression of L-stearoylthreonine methyl ester (L-STME), D-stearoylserine methyl ester (D-SSME), and their mixtures on a pure water subphase at 25.0 °C. % L-STME: A = 0.0% (100.0% D-SSME); B = 25.0%; C = 50.0%; D = 75.0%; E = 100.0% (0.0% D-SSME).

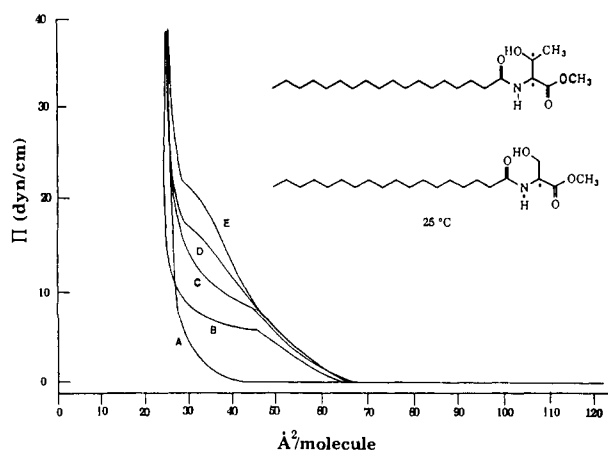


Figure 19. Surface pressure vs area isotherms for the compression of L-*allo*-stearoylthreonine methyl ester (L-*allo*-STME), L-stearoylserine methyl ester (L-SSME), and their mixtures on a pure water subphase at 25.0 °C. % L-*allo*-STME: A = 0.0% (100.0% L-SSME); B = 25.0%; C = 50.0%; D = 75.0%; E = 100.0% (0.0% L-SSME).

STME at 20 °C and a compression rate of 19.24 Å²/molecule/min. Identical results were obtained for mixtures of opposite chirality, i.e., D-STME + D-*allo*-STME and D-STME + L-*allo*-STME. The effects of mixing on the isothermal curve are greater for the latter mixture than for the former mixture, since a com-

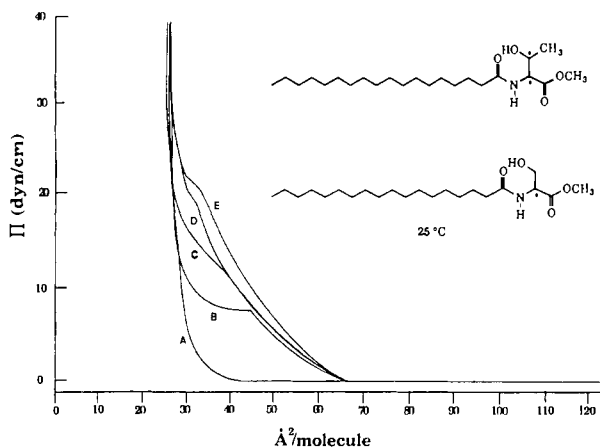


Figure 20. Surface pressure vs area isotherms for the compression of *L-allo*-stearoylthreonine methyl ester (*L-allo*-STME), *D*-stearoylserine methyl ester (*D*-SSME), and their mixtures on a pure water subphase at 25.0 °C. % *L-allo*-STME: A = 0.0% (100.0% *D*-SSME); B = 25.0%; C = 50.0%; D = 75.0%; E = 100.0% (0.0% *D*-SSME).

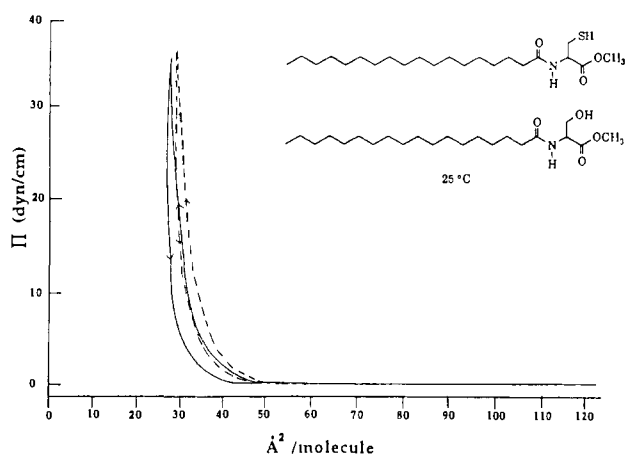


Figure 21. Surface pressure vs area isotherms for the compression of 1/1 mixtures of *L*-stearoylcysteine methyl ester with *L*-stearoylserine methyl ester (---) and *L*-stearoylcysteine methyl ester with *D*-stearoylserine methyl ester (—) on a pure water subphase at 25.0 °C. Arrows indicate direction of compression and expansion.

pletely expanded curve is obtained for *L*-STME + *D-allo*-STME films mixed in a 50/50 ratio.

(2) Mixtures of Two Chiral Surfactants. Figures 17–20 give the compression Π/A isotherms for the four possible diastereomeric combinations of STME/SSME film mixtures. The experiments were done at 25 °C, since at this temperature both STME and SSME films display significant enantiomeric discrimination properties. Cross-chiral checks of these mixed films yielded identical results.

Figure 21 gives the compression/expansion Π/A isotherms for 1/1 mixtures of *L*-stearoylcysteine methyl ester (*L*-SCME) with *L*-SSME and with *D*-SSME at 25 °C, cycled at 19.24 Å²/molecule/min. The *L*-SCME/*L*-SSME mixtures are slightly more expanded than the *L*-SCME/*D*-SSME mixtures, although the isotherm shape is similar for both mixtures.

Stability Limits. The monolayer stability limits for the above diastereomeric mixtures are shown in Table VII. The enantiomers of SCME and SSME and their mixtures form films which are unstable at all surface pressures at 25 °C.

Area Additivities. An assessment of the mixing behavior in *L*-/*meso*-DLCDME monolayers at 25 °C is given in Figure 22, where the area additivities of the mixtures are plotted at surface pressures of 2.5, 5.0, and 7.5 dyn/cm (pressures within their stability limits). There is no deviation (within experimental error) from the dashed line which connects the areas corresponding to pure *L*- and *meso*-DLCDME at each surface pressure, indicating ideal additivity throughout the range of compositions.

Table VII. Monolayer Stability Limits for Spread Films of Various Monolayer Mixtures on a Pure Water Subphase

% L isomer	stability limit (dyn/cm)
L-DLCDME + <i>meso</i>-DLCDME Mixtures at 25 °C	
0	~9
25	~13
50	~18
75	~12
100	~10
L-STME + <i>L-allo</i>-STME Mixtures at 20 °C	
0.0	~8
25.0	~6
50.0	~8
75.0	~7
100.0	~6
L-STME + <i>D-allo</i>-STME Mixtures at 20 °C	
0.0	~8
25.0	~8
50.0	~10
75.0	~9
100.0	~6
L-STME/<i>L</i>-SSME Mixtures at 25 °C	
0.0	0
25.0	~1
50.0	~3
75.0	~4
100.0	~11
L-STME/<i>D</i>-SSME Mixtures at 25 °C	
0.0	0
25.0	~1
50.0	~11
75.0	~6
100.0	~11
<i>L-allo</i>-STME/<i>L</i>-SSME Mixtures at 25 °C	
0.0	0
25.0	~1
50.0	~5
75.0	~7
100.0	~16
<i>L-allo</i>-STME/<i>D</i>-SSME Mixtures at 25 °C	
0.0	0
25.0	~2
50.0	~6
75.0	~7
100.0	~16

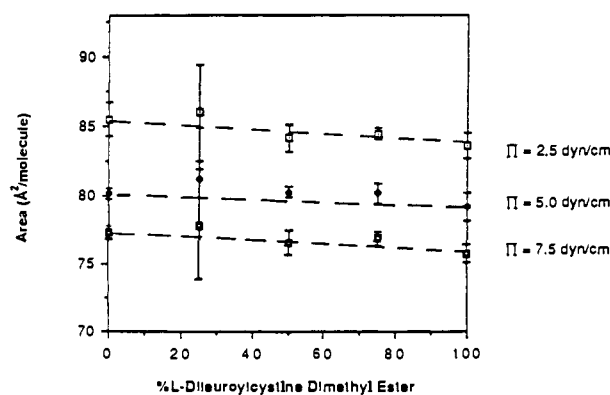


Figure 22. Average molecular area vs film composition for mixtures of *L*- and *meso*-dilauroylcysteine dimethyl esters at 25.0 °C and $\Pi = 2.5, 5.0,$ and 7.5 dyn/cm. The dashed lines correspond to ideal additivity.

The average area per molecule vs composition diagrams for diastereomeric mixtures of STME at 20 °C and $\Pi = 2.5, 5.0,$ and 7.5 dyn/cm are given in Figure 23. Both plots indicate positive deviations from ideality at all surface pressures. The curves drawn through the points are merely a guide to the eye

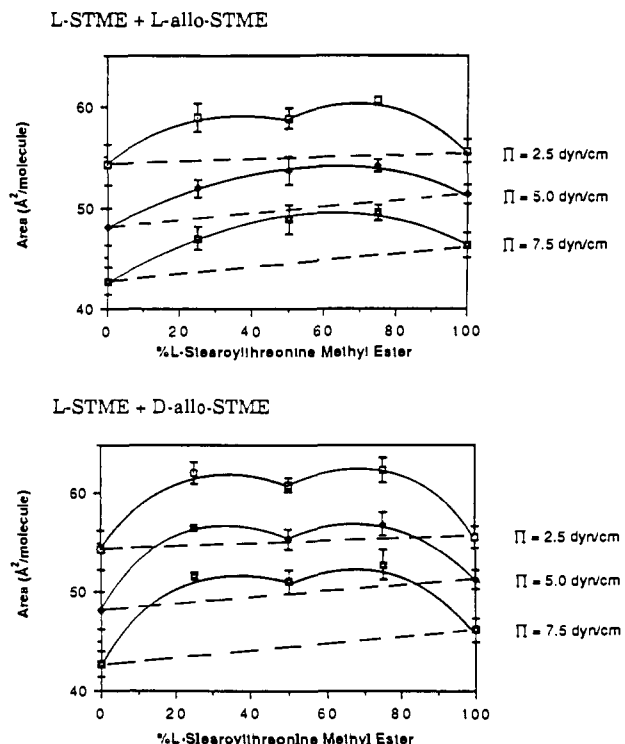


Figure 23. Average molecular area vs film composition for mixtures of L- and L-allo-stearoylthreonine methyl esters (top) and L- and D-allo-stearoylthreonine methyl esters (bottom) at 20 °C and $\Pi = 2.5, 5.0,$ and 7.5 dyn/cm. The dashed lines correspond to ideal additivity.

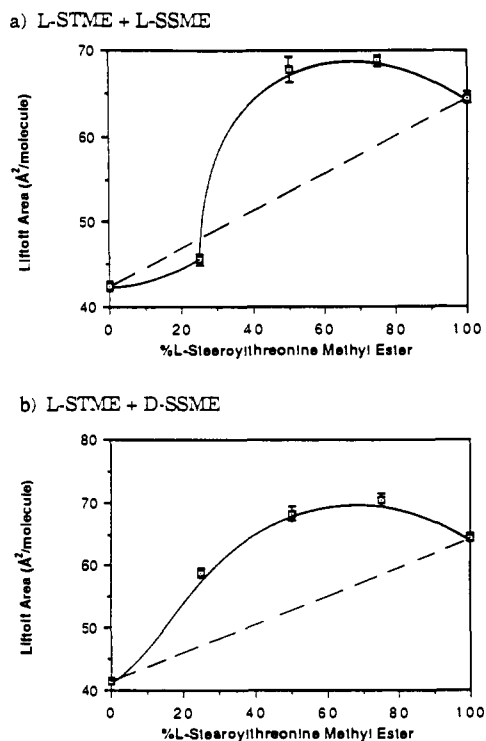


Figure 24. Average molecular area vs film composition for mixtures of (a) L-stearoylthreonine methyl ester (L-STME) with L-stearoylserine methyl ester (L-SSME) and (b) L-STME with D-SSME at 25 °C and $\Pi =$ lift-off area. The dashed lines correspond to ideal additivity.

to relate the areas at different pressures to each other for comparison to ideal behavior.

Area additivities for the STME/SSME mixtures are shown in Figures 24 and 25 at 25 °C and $\Pi =$ lift-off area, the area at which the film first registers a positive surface pressure. The lift-off area represents the point at which measurable chiral discrimination is first observed in enantiomeric and racemic SSME monolayers.⁹

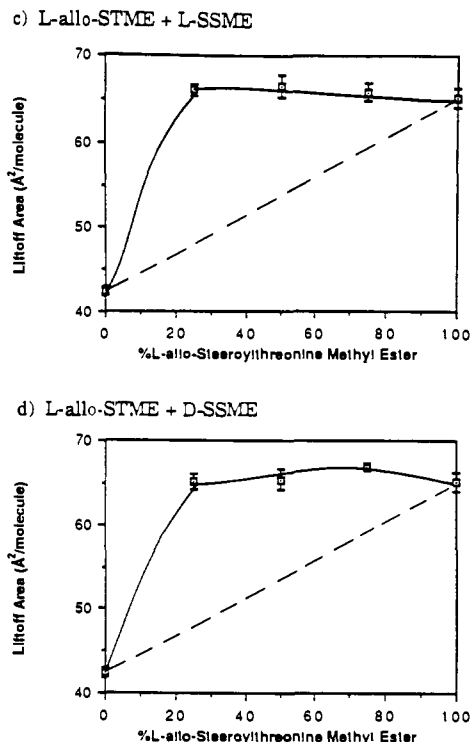


Figure 25. Average molecular area vs film composition for mixtures of (c) L-allo-Stearoylthreonine methyl ester (L-allo-STME) with L-stearoylserine methyl ester (L-SSME) and (d) L-allo-STME with D-SSME at 25.0 °C and $\Pi =$ lift-off area. The dashed lines correspond to ideal additivity.

These plots show predominantly positive deviation from the ideal line.

Discussion

The effects of headgroup structure and temperature on monolayer force–area curves of SCME, DLCDME, STME, and SSME are portrayed in Figures 2–5, respectively. Clearly, intermolecular forces in this state of matter are highly sensitive to the detailed stereochemical structure of the headgroup and to the temperature. Furthermore, as we have emphasized previously,^{9,12,29,30} relaxation processes in compressed monolayers often take place on a slower time scale than the mechanical compression–expansion cycle of the moving barrier on the film balance, which leads to the hysteresis loops observable on several of the Π/A plots. In fact, one might suppose that some of the plots (e.g., DLCDME at 35 °C) are just artifacts or experimental singularities. Here we must emphasize that not only were all curves completely reproducible through numerous replications, but they were repeated completely with the enantiomer of each compound. Hence, even the most complex behavior represents genuine physical phenomena.

As a point of departure for discussing SCME, DLCDME, STME, and the meso and allo diastereomers of the latter two, we refer to the previous study of SSME,⁹ which is the most completely investigated surfactant to date. For that compound, compressed films were examined on the aqueous subphase by the McConnell epifluorescent technique³¹ and also by transmission electron microscopy and scanning tunneling microscopy of films transferred to solid supports by the Langmuir–Blodgett method. By all of these methods, and also those used in the present article, it was concluded there was considerable quasicrystalline order in

(29) Arnett, E. M.; Harvey, N. G.; Rose, P. L. *Acc. Chem. Res.* **1989**, *22*, 131.

(30) Arnett, E. M.; Gold, J. M.; Harvey, N. G.; Johnson, E. A.; Whitesell, L. G. In *Biotechnology Applications of Lipid Microstructures, Advances in Experimental Medicine and Biology*; Gaber, B. C., Schnur, J. M., Chapman, D., Eds.; Plenum: New York, 1988; Vol. 238.

(31) McConnell, H. M.; Tamm, L. K.; Weis, R. M. *Proc. Natl. Acad. Sci. U.S.A.* **1984**, *81*, 3249.

the enantiomeric films compared to highly fluid racemic ones.

Crystal Properties. Significant comparisons could be made between the melting behavior of the SSME crystals as a function of enantiomer composition and a corresponding plot of composition versus the molecular area at liftoff—the point at which the surface pressure begins to rise due to measurable intermolecular repulsions in the monolayer.

For the present compounds, the most useful comparison is between the thermodynamics of fusion (Table VI) and of spreading (Table III) for STME and the same data for SSME. The only difference between these compounds (Figure 1) is that STME carries a methyl group on the same carbon as the hydroxyl group of SSME. This produces another chiral center and hence diastereomers—the pair of enantiomeric allo compounds.

Heats and entropies of fusion refer to the changes of those properties as a crystal is converted to its liquid melt at the fusion point. Heat energy is required to disrupt the ordered structure of the crystal, and there is a gain in entropy. SSME,⁹ SCME (Figure 7), DLCDME (Figure 8), and STME (Figure 9) all give melting point curves which indicate the formation of a racemic compound. However, that for SSME melts at a higher temperature than that of the enantiomers, while those of the other three melt below their enantiomers.

There is virtually no difference between the ΔH°_f and ΔS°_f values for racemic and enantiomeric *allo*-STME, and they are close to the corresponding values for racemic STME, but well below those for enantiomeric STME which requires more heat to melt it and correspondingly gains more entropy. A much larger enantiomer/racemate difference is seen for SSME, whose enantiomeric crystal appears to be more tightly organized presumably because it can enjoy better intermolecular hydrogen bonding in the absence of the added methyl group in STME.

Attribution of the relatively high ΔH°_f and ΔS°_f values of SSME to hydrogen bonding is supported by comparison to SCME, which is its thiol analogue (Table VI). The melting point vs composition diagram for SCME (Figure 7) indicates weakly defined racemate formation at a much lower melting point than the enantiomers, much less heat is required to disrupt the crystals, and much less entropy is gained than for SSME.

The two-chain surfactant, DLDCME, somewhat surprisingly falls into the same range of fusion properties as do the single-chain compounds. It may be regarded as two molecules of SCME bound together through their sulfurs. Yet the enthalpy and entropy changes that accompany the crystal-to-liquid change are scarcely different from those of SCME and also are barely affected by the intramolecular stereochemistry difference in the meso compound.

Comparison of Thermodynamic Properties for Spreading. When a surfactant crystal is placed on a clean water surface its molecules may diffuse off to produce a monolayer. The process is analogous in many ways to the sublimation of a crystal into a gaseous state, and in both cases a true thermodynamic equilibrium may be established. The equilibrium spreading pressure, ESP, is analogous to the sublimation vapor pressure, and thermodynamic properties for spreading may be derived. Since fusion of a crystal to produce its pure liquid phase and spreading to produce a monolayer have the same initial state (but usually at quite different temperatures), it is informative to compare thermodynamic properties for the two types of processes.

Table III provides spreading properties for D-, L-, and *allo*-STME and the racemate of STME. In some cases, values for enantiomeric and racemic SSME,⁹ whose properties are in parentheses in Table III, are given. The thermodynamic spreading properties for the two compounds are remarkably similar, indicating the relatively small effect of attaching the methyl group to the carbon bearing the hydroxyl function in SSME. However, enantiomeric STME would not spread to give a measurable ESP although its racemate and *allo* diastereoisomer would. This difference is probably attributable to a somewhat tighter degree of packing in the crystal since enantiomeric STME has considerably higher ΔH°_f and ΔS°_f values than does its racemate or the *allo* forms (Table VI).

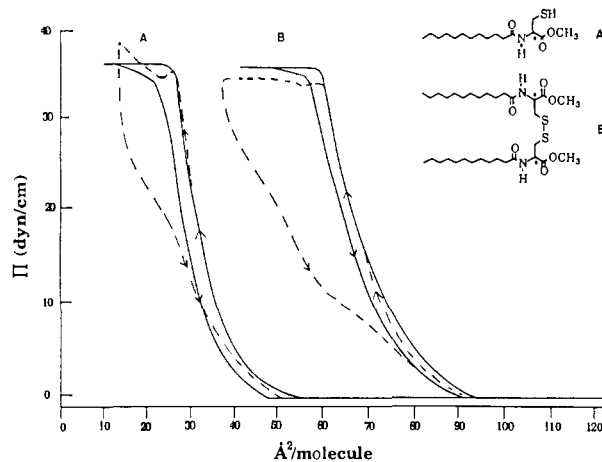


Figure 26. Surface pressure vs area isotherms for the compression and expansion of (A) enantiomeric (---) and racemic (—) lauroylcysteine methyl esters and (B) enantiomeric (---) and meso (—) dilaurolycysteine dimethyl esters at 25.0 °C. Arrows indicate direction of compression and expansion.

Unfortunately, crystalline SCME does not give measurable ESPs, so that no thermodynamic properties for spreading can be derived. However, we may readily infer that an important driving force for the spreading of SSME is the interaction of its hydroxyl group with the aqueous subphase. Since the ΔH°_f and ΔS°_f values for SSME are greater than those of SCME, its crystal is more difficult to convert to the liquid state at its melting point. Still, SSME spreads well, with the racemate forming its monolayer with greater facility than its enantiomers.

All of the spreading properties of two-chain DLDCME (Table II) are significantly higher than those of STME, SSME, and certainly its single-chain analogue SCME, which does not even spontaneously spread from its crystalline state.

It would be most desirable to have definitive structural information about these compounds in their crystalline states. However, as in our previous work,⁹ we were unable to obtain crystals that met the demanding requirements of X-ray studies for long-chain fatty acid derivatives. Also, no directly relevant crystal structures for the amino acids or their derivatives were found—the acids themselves are zwitterionic in the crystalline state.

Force–Area Isotherms. Figures 2–5 present the Π/A plots for monolayers of SCME, DLCDME, and STME at a series of temperatures, with corresponding plots of SSME produced from ref 9. These monolayers were spread, in the usual manner, from solution in an appropriate solvent that dissipates by evaporation or solution in the subphase after spreading. Table IV gives the stability limits for each film in terms of our criterion of being “stable” if the loss of film pressure is less than 0.1 dyn/cm/min. The fact that all of these pressures are above the ESPs at the same temperature is direct evidence that they are metastable with respect to the crystalline state and conforms to the visualization of quasicrystalline surface regions for SSME using the McConnell epifluorescence method.

All four surfactants exhibited hysteresis as the difference between their isotherms under compression and expansion at most temperatures. The greatest is exhibited by DLCDME at 35 °C and the least by STME at 35 °C. Racemic STME and SSME films are more expanded than the enantiomers at all temperatures while the reverse is true for SCME. Complex surface phase behavior is apparent for DLCDME at all four temperatures and can also be seen at several temperatures for STME and SSME, both of which have hydroxyl groups that can hydrogen bond to the surface or, intramolecularly, to the ester or amide function. The phase behavior of SCME is much simpler, presumably because it is a single-chain compound with a poor hydrogen-bonding SH function instead of a hydroxyl group.

An interesting comparison of a single-chain thiol surfactant, lauroylcysteine methyl ester (LCME), with its two-chain disulfide analogue is seen in Figure 26, which shows how faithfully the

behavior of the single-chain system is reproduced by DLCDME, except that the molecular areas for all events for DLCDME occur at slightly less than twice the molecular area as that of LCME.

Surface Shear Viscosities. The modified Verger film balance provided a means to determine the surface shear viscosities by measuring the rates at which films can be forced through a narrow canal at constant pressure—a two-dimensional analogue of an Ostwald viscometer. Viscosities for the various forms of DLCDME and STME at a variety of temperatures and pressures are reported in Table V with a few values for SSME.⁹ Unfortunately, the films of SCME were too unstable to allow this type of experiment.

Enantiomeric SSME was too condensed to give Newtonian flow up at 40 °C, at which point it was sufficiently fluid to be indistinguishable from the racemic modification. DLCDME undergoes Newtonian flow under all conditions shown and exhibits no stereoselection in its flow properties. In contrast, viscosities show chiral discrimination for STME and *allo*-STME films, especially at lower temperatures and higher film pressures. The only data for SSME at 5.0 dyn/cm and 30 °C indicate that it is somewhat more viscous under the same conditions, which one is tempted to relate to the expanding influence of the methyl group on STME reducing cohesive interactions in the monolayer.

Mixed Monolayers. By analogy to the melting point composition diagrams discussed above, we have examined the Π/A curves for various mixtures of the enantiomers of DLCDME at 25 °C (Figure 10) and of STME at 15.5 °C (Figure 12) in order to observe how collapse pressures, Π^{coll} , and transition pressures, Π^{trans} , respond to enantiomeric composition.

The monolayer films for enantiomeric and racemic dilauroylcystine dimethyl ester (DLCDME) exist in a liquid-expanded phase below their collapse pressures (Figure 3). It is essentially these collapse pressures (Π^{coll}) that define the enantiomeric recognition observed in the films, since the Π^{coll} of the racemic film is at least 20 dyn/cm lower than that of the enantiomeric film at all temperatures studied. This recognition is not sensitive to temperature in the 20–35 °C range. Once the films have collapsed, expanding them back to zero surface pressure apparently restores their monolayer character, as they can be recompressed to yield Π/A isotherms identical to their initial curves.

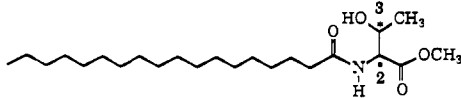
In the sense that the molecules in the DLCDME films are in an expanded state up to their collapse pressures and exist in a solid state thereafter during the compression cycle, this transition is similar to sublimation. The plot of Π^{coll} vs enantiomeric ratio (Figure 11) is reminiscent of that for sublimation of a racemic compound at constant temperature and implies that heterochiral pairing is favored in the films of DLCDME, just as it is in the crystals (Figure 8). Since the transitions take place at surface pressures above the ESPs of the DLCDME crystals (Table II) and above the monolayer stability limits of Table IV, the transition does not involve an equilibrated system and is not modeled exactly by a true sublimation.

Films of STME (Figure 4) show clearly defined phase transitions from 15.5 to 25 °C. Although these monolayers are unstable above Π^{trans} , the slopes of the isotherms are independent of compression rate, and films compressed in the presence of a bulk crystal of the surfactant (a nucleation site) show no difference from those compressed without the crystal present. These observations provide evidence against film collapse during compression, in contrast to those of DLCDME.

The plot of Π^{trans} vs enantiomeric composition for STME (Figures 12 and 13) appears to be similar to a sublimation diagram for a racemic compound at constant temperature, as does that for DLCDME. However, the fact that the plot for STME involves a transition between two monolayer states makes for a tighter analogy to the sublimation process than does the collapse of the DLCDME films.

The isotherms of the mixtures of L(or D)-DLCDME with *meso*-DLCDME (Figure 14) indicate virtually no diastereomeric recognition, except in the collapse behavior. To a *meso* molecule, both L and D enantiomers look the same and are nearly indistinguishable from another *meso*.

Table VIII. Intermolecular Chiral Center Configuration Comparison in Monolayer Films of Stearoylthreonine Methyl Ester (STME) and Correlation with Film Behavior at 20 °C



film	center # 2	center # 3	film behavior
L-STME (2 <i>S</i> ,3 <i>R</i>)	<i>S</i> ·· <i>S</i>	<i>R</i> ·· <i>R</i>	condensed
D,L-STME	<i>S</i> ·· <i>R</i>	<i>R</i> ·· <i>S</i>	expanded
L- <i>allo</i> -STME (2 <i>S</i> ,3 <i>S</i>)	<i>S</i> ·· <i>S</i>	<i>S</i> ·· <i>S</i>	condensed
D,L- <i>allo</i> -STME	<i>S</i> ·· <i>R</i>	<i>S</i> ·· <i>R</i>	expanded
L-STME/L- <i>allo</i> -STME ^a	<i>S</i> ·· <i>S</i>	<i>R</i> ·· <i>S</i>	condensed
L-STME/D- <i>allo</i> -STME ^a	<i>S</i> ·· <i>R</i>	<i>R</i> ·· <i>R</i>	expanded

^a 1/1 mixture.

In contrast, significant diastereomeric interactions are manifested in the mixtures of L-STME and L-*allo*-STME (Figure 15) and even more in those of L-STME with D-*allo*-STME (Figure 16) at 20 °C. Even greater effects are seen for mixtures of L-STME and L-SSME (Figure 17), L-STME and D-SSME (Figure 18), L-SSME and L-*allo*-STME (Figure 19), and D-SSME with L-*allo*-STME (Figure 20). Mixtures of L-SCME with L- and D-SSME at 25 °C (Figure 21) are very similar to those of enantiomeric and racemic SCME at the same temperature (Figure 2) and show none of the phase transitions of SSME (Figure 5).

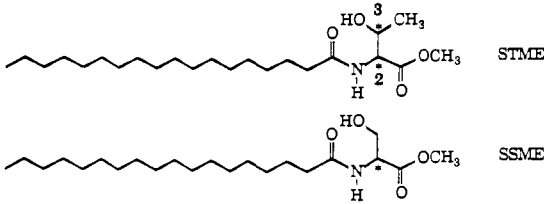
The mechanical mixing of film-forming components in solution does not necessarily lead to completely (or even partially) miscible monolayers once they are spread. The stability limits of “mixed” monolayers can shed light on the question of true miscibility in these films. An increase in stability upon mixing, compared to the less stable of the two pure films, gives evidence for interaction between the species within the monolayer and indicates at least partial miscibility.³² There is a clear enhancement in stability for the mixtures presented in Table VII, indicating some degree of interaction among the two components in the film.

Area additivities provide another method for assessing miscibility in two-component films. The data for DLCDME mixtures (Figure 22) indicate ideal additivity within experimental error, which means that the film components are either completely miscible or completely immiscible at the surface pressures analyzed (which are within the stability limits).

In contrast, Figures 23–25 show positive deviations from ideality, which are clear evidence for intermolecular interactions between the various components to produce greater molecular areas than expected. In the case of the interactions of the enantiomers of SSME with those of SCME, it is reasonable to attribute the behavior to the interference of the thiol function of the latter with the hydrogen bonding of the hydroxyl of SSME to the surface or between its molecules.

Table VIII reveals an interesting correlation relating chiral center configuration and monolayer film phase behavior among the isomers and 1/1 mixtures of isomers of STME. The “*R*” and “*S*” designations refer to Cahn–Prelog–Ingold nomenclature. The dots are meant to imply intermolecular interaction between adjacent centers in the film at either position 2 or 3, as shown in the accompanying structure for STME. The film behavior is classified as “condensed” if the isotherm of the monolayer displays a LE–LC phase transition and “expanded” if the film remains in the LE state throughout compression. In cases where interactions at the number 2 center are homochiral, i.e., interactions are between centers having the same configuration, condensed behavior results. If opportunities for heterochiral interactions exist at this center (an *R* center interacting with an *S* center), the resulting monolayers are expanded. Such a correlation does not hold for interactions involving the number 3 center. This suggests that the chirality at the number 2 center plays a more prominent role in determining phase behavior in the STME films, while

Table IX. Correlation of Film Behavior at 25 °C with Chirality in Mixed Monolayer Films of Stearoylthreonine Methyl Ester (STME) and Stearoylserine Methyl Ester (SSME)



film mixture (1/1)	chirality (STME/SSME)	film behavior
L-STME/L-SSME	2 <i>S</i> ,3 <i>R</i> / <i>S</i>	condensed
L-STME/D-SSME	2 <i>S</i> ,3 <i>R</i> / <i>R</i>	expanded
L- <i>allo</i> -STME/L-SSME	2 <i>S</i> ,3 <i>S</i> / <i>S</i>	condensed
L- <i>allo</i> -STME/D-SSME	2 <i>S</i> ,3 <i>S</i> / <i>R</i>	expanded

chirality at the number 3 center plays a more passive role.

Table IX reveals that for 1/1 mixed films of SSME with STME, behavior similar to the condensed films of Table VIII occurs for mixtures where the chirality at STME center 2 is the same as that in SSME. For cases where the configuration at STME center 2 is opposite to that of SSME, behavior resembling the expanded monolayers of Table VIII occurs.

While the correlations discussed above are suggestive of particular interactions leading to chiral recognition, they do not allow one to get a true picture of what the specific interactions are at a molecular level. Unfortunately, crystal structures of the surfactants of this project could not be obtained, despite several attempts at growing suitable crystalline specimens. The CPK models of each surfactant were constructed, but modeling interactions with these failed to demonstrate any readily interpretable structure/property relationships which could explain the chiral discrimination observed in the surface films uniquely.

Conclusions

The chiral molecular recognition manifested in the monolayer films of the surfactants studied here is strongly phase-dependent, but no simple pattern related to headgroup geometry is apparent. Isotherms of enantiomeric and racemic SCME, in which the molecules of the film are tightly packed at all $\Pi > 0$, are distinct from one another at virtually all surface pressures. In contrast,

the monolayers of DLCDME, which exist in a more expanded phase (liquid-expanded) below their collapse pressure, are independent of stereochemistry in this region.

The STMEs indicate the monolayer transition from the liquid-expanded (LE) to the liquid-condensed (LC) phase as the point at which chiral discrimination is readily detectable in this class of surfactant by the monolayer methods used (Π/A measurements and viscosities). Moreover, this LE-LC phase behavior is highly temperature-dependent in the range of study. Although the intermolecular interactions in the LC phase are obviously tighter than those in the LE phase, the viscosities of the threonine surfactants distinguish the LC phase from a two-dimensional solid, which would show no viscous flow at all.

For none of the surfactants studied was chiral recognition observed in the monolayers at film pressures below the equilibrium spreading pressure. Only in metastable or unstable monolayer states (or collapse states) did differences based on stereochemistry occur.

Comparisons of enantiomeric discrimination between the monolayer films of a particular surfactant and its crystals (where chiral discrimination was always manifested) show that the sense of discrimination is the same in each case, since heterochiral interactions are favored (preference for pairwise interactions between chiral molecules of opposite configuration, rather than for interactions between molecules of the same configuration).

The two-component monolayer mixtures indicate that the degree of diastereomeric recognition is of the same order as the enantiomeric recognition for each surfactant studied. Examination of mixtures of the isomers of STME, and its mixtures with SSME, reveals a trend in film packing that implies that the chiral center α to the ester group (carbon 2) in STME plays a more dominant role than that of carbon 3 in determining the phase behavior, and thus the chiral recognition, observed in its monolayers.

Acknowledgment. We appreciate support for this work by a grant from A.T.&T. to Duke University, and we thank Mrs. Marjorie Richter, Dr. Philip Rose, and Dr. Noel Harvey for invaluable assistance.

Registry No. L-SCME, 122445-68-5; (\pm)-SCME, 140659-83-2; L-DLCDME, 121972-22-3; (\pm)-DLCDME, 140676-29-5; L-STME-(2*S*,3*R*), 101174-52-1; DL-*threo*-STME, 140849-80-5; L-*allo*-STME-(2*S*,3*S*), 140849-81-6; DL-*erythro*-STME, 140849-82-7; L-SSME, 118319-51-0; (\pm)-SSME, 118319-49-6; *meso*-DLCDME, 140850-77-7; D-*allo*-STME(2*R*,3*R*), 140849-83-8; D-SSME, 118319-50-9.

The Anion Radical of Bicyclonatriene

Gerald R. Stevenson,* Richard D. Burton, and Richard C. Reiter

Contribution from the Department of Chemistry, Illinois State University, Normal, Illinois 61761. Received October 28, 1991

Abstract: The low-temperature potassium metal reduction of bicyclo[6.1.0]nona-2,4,6-triene (BCN) in DME leads to the formation of the previously observed open form of the homocyclooctatetraene anion radical (HCOT^{•-}). Careful inspection of the EPR spectra recorded from these solutions, and some of those previously published, shows the presence of another species. This second species is best interpreted using a set of methylene proton coupling constants very similar to those of HCOT^{•-} (all within 10%) but much smaller endo and exo bridgehead coupling constants. Perdeuteriation of the sp^2 carbons supports this interpretation. The only reasonable interpretation of the hyperfine pattern observed for the second anion radical is in terms of the closed (bicyclic) form. The closed anion radical (BCN^{•-}) is favored under conditions involving more ion association and more complete reduction.

In order to account for the high stability of molecules in which conjugation is interrupted in one or more places by aliphatic

groups, some 43 years ago Winstein and Adam¹ extended the concept of aromaticity to include homoaromatic compounds. The